Robust synchronization via maximal monotone couplings

Felix Miranda-Villatoro

Robust synchronization via maximal monotone couplings

Félix A. Miranda-Villatoro

Univ. Grenoble-Alpes, INRIA, LJK, CNRS, 38000 Grenoble, France

Abstract

We explore the use of set-valued coupling laws for the design of robust synchronized behaviors in networks of dynamical systems. Under an incremental dissipativity context, it is shown that coupling systems via maximal monotone mappings leads to synchronization that is robust against both, matched disturbances and changes in the topology of the network. Additionally, it is shown that perfect synchronization of heterogeneous networks with persistent matched disturbances is attained with *finite coupling strength* but *infinite incremental gain* of the coupling maps. The real-life implementation of the proposed controllers is studied under the context of practical synchronization via Yosida regularizations. Simulations illustrate the effectiveness of the proposed methods.

Key words: Maximal monotone maps; incremental passivity; synchronization; nonsmooth dynamical systems; Yosida regularization.

1 Introduction

The study of interacting dynamical systems reaching a common uniform behavior has received numerous attention from the control community in recent years. The problem has been broadly addressed under several scenarios and under different conditions, see *e.g.*, [1], [14], [31], [32], [36], [38], [41] and references therein. Robust synchronization in the presence of disturbances in the individual agents, as well as, in the network connections occupies a special place of interest due to its broad application in several fields. Among the studies dealing with robust synchronization one finds [15], [28], [29], [42]. For instance, in [29] the authors studied practical synchronization of perturbed agents coupled via linear diffusion. It is shown there that the ultimate bound of the synchronization error is inversely proportional to the coupling gain, relying on high-gain couplings as a way of enhancing precision. Nonsmooth coupling laws were analyzed in [13], [15], where sufficient conditions for practical synchronization were provided. Though it is left open if there is any advantage on using nonsmooth coupling schemes, since Assumption 3 in [15] also holds in the case of smooth coupling maps. On the other hand, perturbations in the network topology are regarded in [28], [42] under the context of switching networks. In [42], the assumption of simultaneous triangularization of all the associated Laplacian matrices plays a fundamental role, whereas [28] shows uniform synchronization in a time varying network topology without any triangularization assumption by means of a Common Quadratic Lyapunov Function (CQLF). Both studies handled the case of linear coupling.

The main aim of this paper is to investigate the advantages of *set-valued* coupling, as well as, issues concerning its implementation. The second goal is to show the important role of monotonicity as unifying framework for robust (linear and nonlinear) synchronization strategies such as, linear diffusion, set-valued sliding-mode control, and funnel control, to mention a few.

To this end, we first analyze the robust synchronization of systems against matched persistent disturbances and later against changes in the network topology. In both cases, each agent is described by a Lur'e-type system, whereas the coupling strategy is characterized by a static set-valued map. First, theoretical results are presented regarding perfect synchronization in presence of matched disturbances. It is confirmed that, even in the nonlinear case, perfect synchronization requires infinite (incremental) gain of the involved coupling maps but not infinite coupling gain, as is the case with linear coupling schemes, [29]. The design strategies here allow for a multilayer design. Indeed, the coupling maps are not constrained to be the same everywhere, only maximal monotonicity is required.

Even though some nonsmooth (discontinuous) synchronization strategies have been recently proposed in [15], [13], there are still open issues concerning their implementation. For instance, there are many applications where discontinuous controllers are impermissible, due to the fact that they conduct to the presence of chattering [39]. For such reason, a more realistic approach leading to practical synchronization is presented in Section 5 by means of regularizing the ideal set-valued coupling controller. More specifically, we explore the use of the so-called Yosida regularization. Such practical viewpoint allows us to confirm that, in order to improve the precision, there is a threshold beyond which an increase in the incremental gain of the nonlinear coupling will diminish the synchronization error whilst maintaining the strength of the coupling finite. This is the intrinsic mechanism behind some *weak coupling* strategies such as [23].

This paper is organized as follows. Preliminaries are covered in Section 2, whereas Section 3 presents the problem to deal with and related results on well-posedness of dynamical systems with set-valued feedback laws. Section 4 deals with the perfect asymptotic synchronization of perturbed systems via the design of set-valued maximal monotone coupling laws, and the effects of regularization are analyzed in Section 5. Afterwards, Section 6 deals with perturbations in the networks connections, whereas Section 7 shows another related family of maximal monotone couplings leading to perturbed Moreau's sweeping processes. Finally, conclusions take place at the end of the paper.

Notation

Let $\langle \cdot, \cdot \rangle$ denote the Euclidean inner product in $\mathbb{R}^l$ and $\| \cdot \|$ the corresponding Euclidean norm. The set $\mathcal{B}_r^l(p) := \{q \in \mathbb{R}^l | \|q - p\| \leq r\}$ denotes the closed ball with radius r and center p in $\mathbb{R}^l$. When the dimension of the space is clear from the context we will denote the closed ball simply as $\mathcal{B}_r(p)$. The interior of a set $\mathcal{S} \subset \mathbb{R}^l$ is denoted as $\operatorname{int} \mathcal{S}$, whereas the relative interior is denoted as $\operatorname{rint} \mathcal{S}$. The neighborhood of radius r of a set $\mathcal{S}$ is the set $\mathcal{N}_r(\mathcal{S}) := \{s \in \mathbb{R}^l | \operatorname{dist}(s, \mathcal{S}) < r\}$, where $\operatorname{dist}(s, \mathcal{S})$ denotes the conventional distance function from a point s to a closed convex set $\mathcal{S}$. The matrix I_l denotes the identity matrix in $\mathbb{R}^{l \times l}$. For a matrix $A \in \mathbb{R}^{l \times l}$, $\lambda_{\min}(A)$ and $\lambda_{\max}(A)$ denote the minimum and maximum eigenvalue of A, respectively, whereas $\|A\| = \sqrt{\lambda_{\max}(A^\top A)}$ denotes the spectral norm of A. The generalized condition number of a matrix $A \in \mathbb{R}^{l \times r}$ is the number $\kappa(A) = \|A\| \cdot \|A^\dagger\|$, where $A^\dagger$ denotes the Moore-Penrose generalized inverse of A.

A set-valued map [1] $\mathbf{M} : \mathbb{R}^l \rightrightarrows \mathbb{R}^l$ maps points from $\mathbb{R}^l$ to subsets of $\mathbb{R}^l$. The set $\operatorname{dom}(\mathbf{M}) := \{\eta \in \mathbb{R}^l | \mathbf{M}(\eta) \neq \emptyset\} \subseteq \mathbb{R}^l$ denotes the domain of $\mathbf{M}$; the set $\operatorname{gph}(\mathbf{M}) := \{(\eta, \vartheta) \in \mathbb{R}^l \times \mathbb{R}^l | \vartheta \in \mathbf{M}(\eta)\}$ denotes the graph of $\mathbf{M}$; and the set $\operatorname{rge} \mathbf{M} := \{\vartheta \in \mathbb{R}^l | \exists \eta \in \mathbb{R}^l \text{ such that } \vartheta \in \mathbf{M}(\eta)\}$ denotes the range of $\mathbf{M}$. The inverse of $\mathbf{M}$ is the set-valued map $\mathbf{M}^{-1}$ with $\operatorname{gph}(\mathbf{M}^{-1}) := \{(\vartheta, \eta) \in \mathbb{R}^l \times \mathbb{R}^l | \vartheta \in \mathbf{M}(\eta)\}$.

2 Preliminaries

2.1 Elements from graph theory

In this section we recall standard tools from graph theory used for modeling networks of interacting systems. The interconnection structure of a network of N agents is modeled by a graph $\mathcal{G}(\mathcal{V}, \mathcal{E})$, where $\mathcal{V} = \{v_1, \ldots, v_N\}$ is the set of vertices, $v_i \in \mathcal{V}$ represents the i-th agent, $\mathcal{E} \subset \mathcal{V} \times \mathcal{V}$ is the set of edges. If $\{v_i, v_j\} \in \mathcal{E}$, then the vertices v_i and v_j are *adjacent*. In addition, each edge $\{v_i, v_j\} \in \mathcal{E}$ is *incident* with the vertices v_i and v_j. When the set of vertices and edges is clear from the context we will denote the graph simply as $\mathcal{G}$. Note that, in the set notation used, $\{v_i, v_j\} = \{v_j, v_i\}$, that is, the graph under consideration is *undirected*. Let $v_i, v_j \in \mathcal{V}$, a path of length m from v_i to v_j is a sequence of $m+1$ vertices $\{\nu_k\}_{k=0}^m \subseteq \mathcal{V}$ such that $\nu_0 = v_i$, $\nu_m = v_j$, and $\{\nu_k, \nu_{k+1}\} \in \mathcal{E}$ for $k \in \{0, \ldots, m-1\}$. The graph $\mathcal{G}(\mathcal{V}, \mathcal{E})$ is *connected* if for any pair of distinct vertices $(v_i, v_j) \in \mathcal{V} \times \mathcal{V}$ there exists a path from v_i to v_j. In what follows we set $N = |\mathcal{V}|$ and $E = |\mathcal{E}|$, the number of vertices and edges in the network, respectively. A subgraph $\mathcal{G}'(\mathcal{V}', \mathcal{E}')$ of $\mathcal{G}(\mathcal{V}, \mathcal{E})$, denoted as $\mathcal{G}' \subseteq \mathcal{G}$, is any graph such that $\mathcal{V}' \subseteq \mathcal{V}$ and $\mathcal{E}' \subseteq \mathcal{E}$. A subgraph of $\mathcal{G}$ is called *spanning* subgraph if $\mathcal{V}' = \mathcal{V}$.

For each edge $\epsilon_k = \{v_i, v_j\} \in \mathcal{E}$ a sign to each end of ϵ_k is assigned. Such sign assignation will provide an *orientation* to the graph $\mathcal{G}(\mathcal{V}, \mathcal{E})$. Along all the manuscript, it is assumed that an orientation has been chosen and it is fixed.

[1] *i.e.*, a non-necessarily single-valued map.

Thus, the *oriented* incidence matrix $\Theta \in \mathbb{R}^{N\times E}$ is given as, see *e.g.*, [18],

$$[\Theta]_{i,k} = \begin{cases} +1, & \text{if } v_i \text{ is the positive end of } \epsilon_k; \\ -1, & \text{if } v_i \text{ is the negative end of } \epsilon_k; \\ 0, & \text{otherwise.} \end{cases}$$

If the graph $\mathcal{G}$ has N vertices and c connected components, then any associated incidence matrix has rank $N - c$.

2.2 Maximal monotone maps

A set-valued map $\mathbf{M} : \mathbb{R}^l \rightrightarrows \mathbb{R}^l$, is monotone if for any two pairs $(\eta_1, \vartheta_1), (\eta_2, \vartheta_2) \in \mathrm{gph}(\mathbf{M})$,

$$\langle \eta_1 - \eta_2, \vartheta_1 - \vartheta_2 \rangle \geq 0 \, .$$

In addition, $\mathbf{M}$ is β-strongly monotone if there exists $\beta > 0$ such that

$$\langle \eta_1 - \eta_2, \vartheta_1 - \vartheta_2 \rangle \geq \beta \|\eta_1 - \eta_2\|^2 \, .$$

Furthermore, $\mathbf{M}$ is called maximal monotone if it is monotone and its graph is not strictly contained in the graph of any other monotone map. For instance, the maps $\varphi(\eta) = M\eta$, where M is a square matrix with a positive definite symmetric part; $\varphi(\eta) = |\eta|^r \mathrm{sgn}(\eta)$, where $r > 0$; $\varphi(\eta) = \tanh(\eta)$; $\varphi(\eta) = \frac{\eta}{a-|\eta|}$, for $|\eta| < a$, where $a > 0$; and $\varphi(\eta) = 1 - e^{-\eta}$; are single-valued, monotone, and continuous, therefore also maximal monotone [5]. Other maximal monotone maps comprise the subdifferentials, ∂f, of convex, proper, lower semicontinuous functions [35],

$$\partial f(\eta) = \{\vartheta \in X | \langle \vartheta, \zeta - \eta \rangle \leq f(\zeta) - f(\eta), \text{ for all } \zeta \in \mathbb{R}^l\}.$$

Special cases include the subdifferentials to the absolute value and indicator functions in Figure 1, leading correspondingly, to the set-valued signum map [2] $\mathbf{Sgn} : \mathbb{R} \to [-1, 1]$, such that $\mathbf{Sgn}(0) = [-1, 1]$ and $\mathbf{Sgn}(\eta) = \{\eta/|\eta|\}$ for $\eta \neq 0$, and the normal cone to a closed and convex set $S \subset \mathbb{R}^l$ at the point $\eta \in S$ (also known as hard-thresholding map), given as

$$\mathbf{N}_S(\eta) := \{\vartheta \in X | \langle \vartheta, \zeta - \eta \rangle \leq 0, \text{ for all } \zeta \in S\} \, .$$

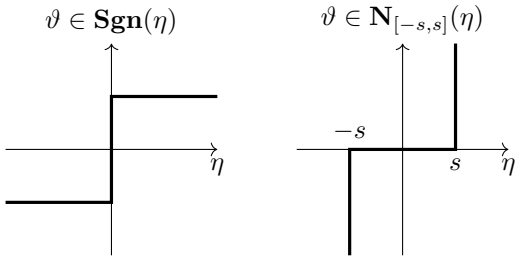

Fig. 1. Set-valued signum and normal cone maps in $\mathbb{R}$.

For a maximal monotone operator $\mathbf{M} : \mathrm{dom}(\mathbf{M}) \rightrightarrows \mathbb{R}^l$, the so-called *Yosida approximation* of index $\varepsilon > 0$, $\mathcal{Y}^{\varepsilon}_{\mathbf{M}} : \mathbb{R}^l \to \mathbb{R}^l$, is the single-valued, Lipschitz continuous function,

$$\vartheta \mapsto \frac{1}{\varepsilon}(\vartheta - \mathcal{J}_{\varepsilon\mathbf{M}}(\vartheta)) \, , \tag{1}$$

where $\mathcal{J}_{\varepsilon\mathbf{M}} : \mathbb{R}^l \to \mathbb{R}^l$ is the so-called resolvant of $\varepsilon\mathbf{M}$, that is,

$$\mathcal{J}_{\varepsilon\mathbf{M}} := (I + \varepsilon\mathbf{M})^{-1} \, , \tag{2}$$

[2] Note that, although discontinuous functions can be monotone, they are not maximal.

which is single-valued and firmly non-expansive [5]. It follows from (1) that for any $\varepsilon > 0$, and any $\vartheta \in \mathbb{R}^l$

$$\vartheta = \mathcal{J}_{\varepsilon \mathbf{M}}(\vartheta) + \varepsilon \mathcal{Y}^{\varepsilon}_{\mathbf{M}}(\vartheta) \ . \tag{3}$$

Moreover, it follows directly from (2) and the definition of $\mathcal{Y}^{\varepsilon}_{\mathbf{M}}$ that for any $\varepsilon > 0$ and any $\vartheta \in \mathbb{R}^l$,

$$\mathcal{Y}^{\varepsilon}_{\mathbf{M}}(\vartheta) \in \mathbf{M}\left(\mathcal{J}_{\varepsilon \mathbf{M}}(\vartheta)\right) \ . \tag{4}$$

3 Problem formulation and well-posedness of Lur'e networks with monotone coupling

We consider an ensemble of N dynamical systems, where the k-th agent (denoted as $v_k \in \mathcal{V}$), is a perturbed Lur'e-type dynamical system given by

$$v_k : \begin{cases} \dot{x}_k(t) = Ax_k(t) - B_1\varphi(y_k(t)) \\ \qquad\qquad + B_2\left(u_k(t) + \xi(t, x(t))\right) \ , \\ y_k(t) = C_1 x_k(t) \ , \\ w_k(t) = C_2 x_k(t) \ . \end{cases} \tag{5}$$

where $x_k(t) \in \mathbb{R}^n$ is the state of the k-th agent; $y_k(t) \in \mathbb{R}^m$ is an (internal) variable used only by the k-th agent; $u_k(t), w_k(t) \in \mathbb{R}^p$ are, respectively, the input and output used to exchange information with other agents; and $\xi_k : \mathbb{R} \times \mathbb{R}^n \to \mathbb{R}^m$ is an unknown function accounting for unmodeled dynamic effects, as well as, external disturbances affecting the system. The map $\varphi : \mathbb{R}^m \to \mathbb{R}^m$ is assumed Lipschitz continuous, satisfying extra conditions stated below. Finally, the matrices A, B_i, and C_i, $i \in \{1, 2\}$, are constant and of the appropriate dimensions.

In this work the following standing assumptions are considered.

Assumption 1 *Each function $\xi_k : \mathbb{R} \times \mathbb{R}^n \to \mathbb{R}^m$ is Lipschitz continuous in the second argument and the map $t \mapsto \xi_k(t, x(t))$ is measurable and uniformly bounded in $\mathcal{L}^\infty[\mathbb{R}_+; \mathbb{R}^m]$, for all $k \in \{1, \ldots, N\}$.*

Assumption 2 *The map $\varphi : \mathbb{R}^m \to \mathbb{R}^m$ is such that for any two $\eta, \tilde{\eta} \in \mathbb{R}^m$, the following incremental sector condition holds:*

$$\left(\Delta\varphi - K_1\Delta\eta\right)^\top \left(\Delta\varphi - K_2\Delta\eta\right) \leq 0,$$

Equivalently,

$$\begin{bmatrix} \Delta\eta \\ \Delta\varphi \end{bmatrix}^\top \begin{bmatrix} K_1^\top K_2 + K_2^\top K_1 & (K_1 + K_2)^\top \\ K_1 + K_2 & 2I_m \end{bmatrix} \begin{bmatrix} \Delta\eta \\ \Delta\varphi \end{bmatrix} \leq 0 \tag{6}$$

where $\Delta\eta = \eta - \tilde{\eta}$, $\Delta\varphi = \varphi(\eta) - \varphi(\tilde{\eta})$, $K_1, K_2 \in \mathbb{R}^{m \times m}$ are diagonal matrices such that $0 \prec K_2 - K_1$.

Functions φ satisfying the incremental sector condition (6) include "N"-shape functions, incrementally passive maps, functions with lack of monotonicity, etc. Thus, the family of Lur'e systems into consideration include, FitzHugh-Nagumo systems, Chua's circuits, Negative resistance oscillators, etc. and is general enough to show bistable, oscillatory or chaotic behavior for instance.

As is usual in the study of systems with output feedback, as is the case of dissipative systems, we impose a detectability assumption as in [34].

Assumption 3 *The incremental dynamics is asymptotically zero-state detectable. That is, for any two systems v_a, v_b such that the output mismatch $w_a(t) - w_b(t) \to 0$, whereas the inputs $\tilde{u}_r(t) = u_r(t) + \xi_r(t)$, $r \in \{a, b\}$ satisfy $\tilde{u}_a(t) \to 0$, $\tilde{u}_b(t) \to 0$ implies $x_a(t) - x_b(t) \to 0$.*

The overall dynamics of the collection of agents is written in compact form as

$$\begin{cases} \dot{x}(t) = (I_N \otimes A)x(t) - (I_N \otimes B_1)\Phi(y(t)) \\ \qquad\qquad + (I_N \otimes B_2)(u(t) + \xi(t, x(t))) \ , \\ y(t) = (I_N \otimes C_1)x(t) \ , \\ w(t) = (I_N \otimes C_2)x(t) \ , \end{cases} \tag{7}$$

where $x(t) \in \mathbb{R}^{Nn}$, $y(t) \in \mathbb{R}^{Nm}, u(t), w(t), \xi(t,x(t)) \in \mathbb{R}^{Np}$ are the collective variables with components $x(t) = [x_1(t)^\top, \dots, x_N(t)^\top]^\top$, (resp. $y(t) = [y_1(t)^\top, \dots, y_N(t)^\top]^\top$, $u(t) = [u_1(t)^\top, \dots, u_N(t)^\top]^\top$, $w(t) = [w_1(t), \dots, w_N(t)]^\top$, $\xi(t,x) = [\xi_1(t,x)^\top, \dots, \xi_N(t,x)^\top]^\top$.) and the aggregated map $\Phi : \mathbb{R}^{Nm} \to \mathbb{R}^{Nm}$ is such that $y \mapsto [\varphi(y_1)^\top, \dots, \varphi(y_N)^\top]^\intercal$. In what follows, a double subindex as $x_{k,i}$, denotes the i-th component of the state of the k-th system, whereas a single index as x_k, denotes the complete state of the k-th system. A similar notation holds for the signals $u(t), w(t), y(t)$ and $\xi(t)$. It is worth to remark that in (7), the coupling law $u(t)$ is the one that encodes the interactions between systems.

Let $\mathcal{G}(\mathcal{V}, \mathcal{E})$ be a connected graph indicating the neighbors to which eah agent is able of exchanging information and let $\Theta \in \mathbb{R}^{N \times E}$ be an oriented incidence matrix of $\mathcal{G}$. Then Θ has rank $N-1$ and null $(\Theta^\top) = \text{rge}\,(\mathbf{1}_N)$. Intuitively, asymptotic synchronization is achieved when there is a coupling law $u(t)$ such that

$$\text{dist}\,(x(t); \text{rge}\,(\mathbf{1}_N \otimes I_n)) \to 0 \text{ as } t \to \infty\,,$$

that is, the mismatch $x_i(t) - x_j(t) \to 0$ as $t \to \infty$, for all $i, j \in \{1, \dots, N\}$. The following definition formalizes such intuition.

Definition 4 *Let $\mathcal{S} = \text{rge}\,(\mathbf{1}_N \otimes I_n)$ be the synchronization manifold. The network (7) achieves*

- *i) asymptotic synchronization if*
  - *(a) for any $0 < \varepsilon$ there exists $0 < \delta = \delta(\varepsilon)$ such that $\text{dist}(x_0, \mathcal{S}) < \delta$ implies $\text{dist}(x(t), \mathcal{S}) < \varepsilon$, for all $t \geq t_0$;*
  - *(b) there exists $s > 0$ such that for any $x_0 \in \mathcal{B}_s(0)$, $\text{dist}(x(t), \mathcal{S}) \to 0$ as $t \to \infty$.*
- *ii) practical asymptotic synchronization if there exist a vector of parameters $p \in \mathbb{R}^{n_p}$ and a continuous positive function $r : \mathbb{R}^{n_p} \to \mathbb{R}_+$ such that*
  - *(a) for any $0 < \varepsilon$ there exists $0 < \delta = \delta(\varepsilon, p)$ such that $\text{dist}(x_0, \mathcal{N}_{r(p)}(\mathcal{S})) < \delta$ implies that $\text{dist}(x(t), \mathcal{N}_{r(p)}(\mathcal{S})) < \varepsilon$ for all $t \geq t_0$;*
  - *(b) there exists $s > 0$ such that for any $x_0 \in \mathcal{B}_s(0)$, $\text{dist}(x(t); \mathcal{N}_{r(p)}(\mathcal{S})) \to 0$ as $t \to \infty$;*
  - *(c) $r(p) \to 0$ as $\|p\| \to \infty$.*

The property is global if it holds for all $x_0 \in \mathbb{R}^{Nn}$ and semi-global if there exists a vector of parameters $q \in \mathbb{R}^{n_q}$ and a continuous positive functions $s : \mathbb{R}^{n_q} \to \mathbb{R}_+$ such that it holds for all $x_0 \in \mathcal{B}_{s(q)}(0)$ and $s(q) \to \infty$ as $\|q\| \to \infty$.

Equivalently, the network (7) achieves global (semi-global, practical) asymptotic synchronization if and only if the zero solution associated to the dynamics of the *spatial* increments $\Delta x := (\Theta^\top \otimes I_n)x \in \mathbb{R}^{En}$ is globally (semi-globally, practically) asymptotically stable.

Problem formulation Let $\mathcal{G}(\mathcal{V}, \mathcal{E})$ be a given undirected and connected graph fixing the network structure. Our target consists in designing a coupling law $u(t)$ that only uses the information of neighbors indicated by the graph $\mathcal{G}(\mathcal{V}, \mathcal{E})$, such that the network (7) achieves robust synchronization in the presence of matched disturbances and/or switching topology.

It is well known that under the presence of persistence disturbances, such as ξ in (7), only practical synchronization is possible via linear couplings. Moreover, the coupling gain is the parameter controlling the size of the ultimate bound, so that $\text{dist}(x; \mathcal{S}) \to 0$ as γ, the coupling gain, increases up to infinity, see *e.g.* [29]. In order to achieve robust synchronization with bounded gains, we focus on coupling laws characterized by strongly monotone maps. Specifically, we consider the coupling law,

$$u(t) \in -(\Theta_a W \Theta_a^\top \otimes I_p)w(t) - \gamma(\Theta_b \otimes I_p)\mathbf{M}\left((\Theta_b^\top \otimes I_p)w(t)\right)\,, \tag{8}$$

where $\gamma > 0$; $W \in \mathbb{R}^{E_a \times E_a}$ is a diagonal matrix with $\min([W]_{i,i}) = \beta > 0$; $\mathbf{M} : \text{dom}(\mathbf{M}) \subseteq \mathbb{R}^{E_b p} \rightrightarrows \mathbb{R}^{E_b p}$ is such that $\mathbf{M} = \mathbf{m}_1 \times \cdots \times \mathbf{m}_{E_b}$, and $\mathbf{m}_j : \text{dom}(\mathbf{m}_j) \subseteq \mathbb{R}^p \rightrightarrows \mathbb{R}^p$ is maximal monotone, for $j \in \{1, \dots, E_b\}$. The matrices $\Theta_a \in \mathbb{R}^{N \times E_a}$ and $\Theta_b \in \mathbb{R}^{N \times E_b}$ are, non-necessarily equal, oriented incidence matrices, both with rank $N-1$ associated, respectively, to the spanning subgraphs $\mathcal{G}_a(\mathcal{V}, \mathcal{E}_a) \subseteq \mathcal{G}$ and $\mathcal{G}_b(\mathcal{V}, \mathcal{E}_b) \subseteq \mathcal{G}$. That is, the coupling law (8) induces a multi-edge structure between vertices, (sometimes known as multi-layer or multiplex network, see *e.g.*, [8], [19]), where the sub-network $\mathcal{G}_a$ is driven by linear diffusion, whereas $\mathcal{G}_b$ is driven by the set-valued coupling law. Even though we are considering only two layers, the developments that follow easily extend to the case of several

layers. It is noteworthy that $\mathbf{M} = I$, the identity map, is maximal β-strongly monotone with $\beta = 1$, and in that case the coupling strategy (8) reduces to the classical linear diffusion coupling. An additional constraint regarding $\mathbf{M}$ is stated below in Section 4. The well-posedness of the interconnected system (7)-(8) is a consequence of the following theorem.

Theorem 5 *Consider the following differential inclusion,*

$$\dot{x}(t) \in h(t, x(t)) - \mathbf{F}(x(t)) \tag{9}$$

where $h : \mathbb{R}_+ \times \mathbb{R}^l \to \mathbb{R}^l$ is a Lipschitz continuous function in its second argument and such that the map $t \mapsto h(t, x) \in \mathcal{L}^\infty[\mathbb{R}_+; \mathbb{R}^l]$, $\mathbf{F} : \mathrm{dom}(\mathbf{F}) \subseteq \mathbb{R}^l \rightrightarrows \mathbb{R}^l$ is a maximal monotone map such that $\mathrm{int}\,(\mathrm{dom}(\mathbf{F})) \neq \emptyset$. Then, for any initial condition $x(t_0) = x_0 \in \mathrm{dom}(\mathbf{F})$, there exists a unique absolutely continuous function $\chi(t, x_0)$ satisfying (9) for almost all times $t \geq t_0$.

For a proof of Theorem 5 the reader is addressed to [9, Proposition 3.13] and [2, Theorem 2.1], see also, [3, Remark 4.1 and Theorem 4.8], and [4, Proposition 2.1] for similar results. The following corollary is an adaptation of Theorem 2 in [10] and state sufficient conditions guaranteeing the existance and uniqueness of solutions for the entire network of agents with maximal monotone coupling laws.

Corollary 6 *Assume that there exists a matrix $P = P^\top \succ 0$ such that $PB_2 = C_2^\top$ and $\mathrm{rge}\,(\Theta_b^\top \otimes C_2 P^{-1/2}) \cap \mathrm{rint}\,(\mathrm{dom}(\mathbf{M})) \neq \emptyset$. Then, for any initial condition $x(t_0) = x_0$ satisfying $(\Theta_b^\top \otimes C_2)x_0 \in \mathrm{dom}(\mathbf{M})$ there exists a unique absolutely continuous function $\chi(t, x_0)$ satisfying (7)-(8) for almost all times $t \geq t_0$.*

PROOF. Consider the change of coordinates $z = (I_N \otimes P^{1/2})x$, then (7)-(8) becomes:

$$\dot{z} \in h(t, z) - (\Theta_b \otimes P^{1/2} B_2)\mathbf{M}\left((\Theta_b^\top \otimes C_2 P^{-1/2})z\right)$$

where

$$\begin{aligned} h(t, z) = {} & (I_N \otimes P^{1/2} A P^{-1/2})z - (I_N \otimes P^{1/2} B_1)\Phi\left((I_N \otimes C_1 P^{-1/2})z\right) \\ & + (I_N \otimes P^{1/2} B_2)\xi\left(t, (I_N \otimes P^{-1/2})z\right) - \left(\Theta_a W \Theta_a^\top \otimes P^{1/2} B_2 C_2 P^{-1/2}\right) z \end{aligned}$$

satisfies the conditions stated in Theorem 5. Now, it follows from the hypothesis in P and [35, Theorem 12.43] that $\mathbf{F} = (\Theta_b \otimes P^{1/2} B_2) \circ \mathbf{M} \circ (\Theta_b^\top \otimes C_2 P^{-1/2})$ is also maximal monotone, and the conclusion follows as a direct consequence of Theorem 5.

It is noteworthy that Corollary 6 allows coupling consisting of unbounded set-valued maps, as for instance, the normal cone in Figure 1, and in such cases, the resulting differential inclusion is not of Filippov type, see *e.g.,* [17]. Thus, the maximal monotone framework allows us to consider more general couplings than, for instance, those studied in conventional sliding mode control.

4 Perfect synchronization via set-valued maximal monotone couplings

In this section it is shown that the coupling strategy (8) achieves asymptotic synchronization with a finite coupling γ in the presence of matched disturbances. To that end, we consider the following assumption on the set-valued map $\mathbf{M}$ in (8).

Assumption 7 *There exists $\rho_{\mathbf{M}} > 0$ such that the maximal monotone map $\mathbf{M}$ in (8) satisfies*

$$\mathcal{B}_{\rho_{\mathbf{M}}}(0) \subset \mathrm{int}\,\mathbf{M}(0)\,. \tag{10}$$

Note that (10) implies that $\mathbf{M}(0)$ is neither empty nor a singleton. In particular, linear coupling maps are excluded in the layer $\mathcal{G}_b$.

The following theorem states that maximal monotone set-valued maps can achieve perfect asymptotic synchronization with finite coupling gain γ.

Theorem 8 *Let Assumptions 1-2 and 7 hold. Let the initial condition $x(t_0) = x_0$ be such that $(\Theta_b^\top \otimes C_2)x_0 \in \mathrm{dom}(\mathbf{M})$, and let $0 < \overline{\xi}$ be such that $\|\xi_k(t, x(t))\| \leq \overline{\xi}$ for all $k \in \{1, \dots N\}$ and for almost all $t \geq t_0$. If*

i) there exist $\mu > 0$ and a matrix $P = P^\top \succ 0$ satisfying the conditions of Corollary 6, together with

$$\begin{bmatrix} \tilde{Q}_1 + \mu P & PB_1 - C_1^\top (K_1 + K_2)^\top \\ B_1^\top P - (K_1 + K_2)C_1 & -2I_m \end{bmatrix} \prec 0 \,, \tag{11}$$

where $\tilde{Q}_1 = A^\top P + PA - 2\beta\lambda_a C_2^\top C_2 - C_1^\top (K_1^\top K_2 + K_2^\top K_1)C_1$ and λ_a is the second smallest eigenvalue of the Laplacian $L_a = \Theta_a \Theta_a^\top$; and

ii) the gain $\gamma > 0$ is such that

$$\gamma > \frac{\overline{\xi}\|H_b\|}{\rho_{\mathbf{M}}} \,, \tag{12}$$

where $H_b \in \mathbb{R}^{E_b \times E_c}$ is a full row-rank matrix such that $\Theta_c = \Theta_b H_b$, see Lemma 17.i) in the appendix.

Then, the perturbed network (7) with coupling law (8) achieves global asymptotic synchronization.

PROOF.

Let us consider the Lyapunov function candidate,

$$V(x) = \frac{1}{2N} x^\top (\Theta_c \Theta_c^\top \otimes P)x \,, \tag{13}$$

where $P = P^\top \succ 0$ satisfies all assumptions of the theorem and $\Theta_c \in \mathbb{R}^{N \times E_c}$, $E_c = \frac{N(N-1)}{2}$, is an oriented incidence matrix associated to the complete graph $\mathcal{K}_N$. Note that $V(x) = 0$ if and only if x lies inside the synchronization manifold $\mathcal{S} = \mathrm{rge}\,(\mathbf{1}_N \otimes I_n)$. Computing the time derivative of V along the trajectories of (7) with coupling (8) yields

$$\begin{aligned} \frac{d}{dt}V(x) \leq \frac{1}{2N} x^\top (\Theta_c \Theta_c^\top \otimes A^\top P + PA)x - \frac{1}{N} x^\top (\Theta_c \Theta_c^\top \otimes PB_1)\Phi(y) + \frac{1}{N}\|(\Theta_c^\top \otimes I_p)w\|\|(\Theta_c^\top \otimes I_p)\xi\| \\ - w^\top (\Theta_a W \Theta_a^\top \otimes I_p)w - \gamma w^\top (\Theta_b \otimes I_p)\vartheta_b \end{aligned} \tag{14}$$

where, $\vartheta_b \in \mathbf{M}\left((\Theta_b^\top \otimes I_p)w\right)$ and we have used Lemma 17 to obtain the last two terms. Now, recalling that $\min_i([W]_{i,i}) = \beta$, it follows that,

$$\begin{aligned} w^\top (\Theta_a W \Theta_a^\top \otimes I_p)w &\geq \beta w^\top (\Theta_a^\top \Theta_a \otimes I_p)w \\ &= \frac{\beta}{N^2} \tilde{w}^\top (\Theta_a \Theta_a^\top \otimes I_p)\tilde{w} \end{aligned}$$

where $\tilde{w} = (\Theta_c \Theta_c^\top \otimes I_p)w$ by the use of Lemma 17. Note that $\tilde{w} \perp \mathrm{rge}\,(\mathbf{1}_N \otimes I_p)$. Indeed, for any $r \in \mathbb{R}^p$

$$\tilde{w}^\top (\mathbf{1}_N \otimes I_p)r = w^\top (\Theta_c \Theta_c^\top \mathbf{1}_N \otimes I_p)r = 0 \,.$$

Hence, setting λ_a as the connectivity of the subgraph $\mathcal{G}_a$, it follows from the Courant-Fisher minimax theorem [20, Theorem 4.2.6] that,

$$w^\top (\Theta_a W \Theta_a^\top \otimes I_p)w \geq \frac{\beta}{N^2}\lambda_a \tilde{w}^\top \tilde{w} = \frac{\beta\lambda_a}{N} x^\top \left(\Theta_c \Theta_c^\top \otimes C_2^\top C_2\right) x \,. \tag{15}$$

Making use of (15) together with Lemma 18.i), (see Appendix), back into (14) leads us to,

$$\frac{d}{dt}V(x) \leq \frac{1}{2N}x^\top \left(\Theta_c\Theta_c^\top \otimes Q_1\right) x - \frac{1}{N}x^\top(\Theta_c\Theta_c^\top \otimes PB_1)\Phi(y) - \gamma\rho_{\mathbf{M}}\|(\Theta_b^\top \otimes I_p)w\| + \frac{1}{N}\|(\Theta_c^\top \otimes I_p)w\|\|(\Theta_c^\top \otimes I_p)\xi\| , \tag{16}$$

where $Q_1 := (A^\top P + PA - 2\beta\lambda_a C_2^\top C_2)$. It follows from simple calculations that

$$\|(\Theta_c^\top \otimes I_p)\xi\| \leq N\,\overline{\xi} \tag{17}$$

$$\|(\Theta_c^\top \otimes I_p)w\| \leq \|H_b\|\|(\Theta_b^\top \otimes I_p)w\| \tag{18}$$

Hence, substitution of (17)-(18) into (16) and rearranging terms leads us to

$$\frac{d}{dt}V(x) \leq \frac{1}{2N}x^\top \left(\Theta_c\Theta_c^\top \otimes Q_1\right) x - \frac{1}{N}x^\top(\Theta_c\Theta_c^\top \otimes PB_1)\Phi(y) - \left(\gamma\rho_{\mathbf{M}} - \overline{\xi}\|H_b\|\right)\|(\Theta_b^\top \otimes I_p)w\| \tag{19}$$

Now we turn to the incremental sector condition (6). Noticing that each row of $\Theta_c^\top$ has exactly two non-zero entries given by $+1$ and -1, it follows from (6) that

$$0 \leq -\frac{1}{2N}\begin{bmatrix}\Delta_c^n x\\ \Delta_c^m\Phi\end{bmatrix}^\top \begin{bmatrix}I_{E_c}\otimes D_1 & I_{E_c}\otimes D_2^\top\\ I_{E_c}\otimes D_2 & 2I_{E_c m}\end{bmatrix}\begin{bmatrix}\Delta_c^n x\\ \Delta_c^m\Phi\end{bmatrix}. \tag{20}$$

where $\Delta_c^n x = (\Theta_c^\top \otimes I_n)x$, $\Delta_c^m\Phi = -(\Theta_c^\top \otimes I_m)\Phi(y)$, $D_1 = C_1^\top(K_1^\top K_2 + K_2^\top K_1)C_1$, and $D_2 = (K_1+K_2)C_1$. Hence, the addition of (19) and (20) leads us to,

$$\frac{d}{dt}V(x) \leq \frac{1}{2N}\begin{bmatrix}\Delta_c^n x\\ \Delta_c^m\Phi\end{bmatrix}^\top \begin{bmatrix}I_{E_c}\otimes \tilde{Q}_1 & I_{E_c}\otimes \tilde{Q}_2\\ I_{E_c}\otimes \tilde{Q}_2^\top & -2I_{E_c m}\end{bmatrix}\begin{bmatrix}\Delta_c^n x\\ \Delta_c^m\Phi\end{bmatrix} - \left(\gamma\rho_{\mathbf{M}} - \overline{\xi}\|H_b\|\right)\|(\Theta_b^\top \otimes I_p)w\| \tag{21}$$

where $\tilde{Q}_1$ is as in (11) and $\tilde{Q}_2 = PB_1 - D_2^\top$. It thus follows from (11) and (12) that $\frac{d}{dt}V(x) \leq -\mu V(x)$. Finally, recalling that $V(x) = 0$ if and only if $x \in \operatorname{rge}(\mathbf{1}_N \otimes I_n)$, global asymptotic synchronization (with a rate of convergence of at least μ) follows.

Note that both, the matrix W and the gain γ are bounded, as opposed to linear designs, where perfect synchronization can only be attained with infinite gains [29], [43]. By contrast, set-valued maps can achieve perfect asymptotic synchronization with finite coupling strength. However, Assumption 7 implies that the coupling map has infinite incremental gain. In the following subsection we study how the implementable controller has an intrinsic limitation in precision that comes from the regularization and not from the magnitude of the coupling gains.

Remark 9 *It follows from the proof of Theorem 8 that, in order to mitigate the affections caused by matched disturbances, it is sufficient for the set-valued coupling induced by* $\mathbf{M}$ *to act on a connected network. For instance,* $\mathcal{G}_b$ *can be a generating tree of the graph* $\mathcal{G}$ *or any simple chain of vertices. This observation allows us to deliver control strategies requiring less cost of energy and implementation, as opposed to those that act on the entire network induced by* $\mathcal{G}$*, see Example 12 below.*

The conditions in Theorem 8 can be relaxed to get a semi-global version as stated in the following corollary.

Corollary 10 *Let Assumptions 1-3 and 7 hold. Moreover, let the initial condition* $x(t_0) = x_0 \in \mathbb{R}^{Nn}$ *be such that* $(\Theta_b^\top \otimes C_2)x_0 \in \operatorname{dom}(\mathbf{M})$ *and for some* $c > 0$*,*

$$x_0 \in \operatorname{int}\Omega_c := \{x \in \mathbb{R}^{Nn} | V(x) \leq c\} . \tag{22}$$

If

i) there exist matrices $R = R^\top$, such that $\lambda_{\max}(R) > 0$, and $P = P^\top \succ 0$ satisfying the conditions of Corollary 6 together with

$$\begin{bmatrix} \tilde{Q}_1 - C_2^\top R C_2 & PB_1 - C_1^\top (K_1 + K_2)^\top \\ B_1^\top P - (K_1 - K_2) C_1 & -2I_m \end{bmatrix} \preceq 0 \,, \tag{23}$$

where $\tilde{Q}_1$ is the same as in Theorem 8; and

ii) the gain $\gamma > 0$ is such that

$$\gamma > \frac{\|H_b\|}{\rho_{\mathbf{M}}} \left(\overline{\xi} + \frac{\sqrt{c}\lambda_{\max}(R)\|C_2\|\kappa(H_b)}{2N\sqrt{\lambda_{\min}(P)}} \right) \tag{24}$$

Then the perturbed network (7) *with monotone coupling* (8) *achieves semi-global asymptotic synchronization.*

PROOF. Taking the same Lyapunov function candidate as in the proof of Theorem 8 we arrive at (21). Hence, it follows from (23) that

$$\begin{aligned} \frac{d}{dt}V(x) &\leq \frac{1}{2N} x^\top (\Theta_c \Theta_c^\top \otimes C_2^\top R C_2) x - \left(\gamma \rho_{\mathbf{M}} - \overline{\xi}\|H_b\|\right) \|(\Theta_b^\top \otimes I_p) w\| \\ &\leq \frac{\lambda_{\max}(R)\|H_b\|^2}{2N} \|(\Theta_b^\top \otimes I_p) w\|^2 - \left(\gamma \rho_{\mathbf{M}} - \overline{\xi}\|H_b\|\right) \|(\Theta_b^\top \otimes I_p) w\| \end{aligned} \tag{25}$$

By assumption $x_0 \in \operatorname{int} \Omega_c$. Hence, there exists $t_1 > t_0$ such that for all $t \in [t_0, t_1]$, $x(t) \in \Omega_c$. Thus, for $t \in [t_0, t_1]$ one has that

$$\begin{aligned} \|(\Theta_b^\top \otimes I_p) w\|^2 &= x^\top \left(\Theta_b \Theta_b^\top \otimes C_2^\top C_2\right) x \\ &\leq \frac{\lambda_{\max}(C_2^\top C_2) x^\top \left(\Theta_c \Theta_c^\top \otimes P\right) x}{\lambda_{\min}(H_b H_b^\top)\lambda_{\min}(P)} \\ &\leq \frac{\|C_2\|^2 \|H_b^\dagger\|^2 c}{\lambda_{\min}(P)} \end{aligned} \tag{26}$$

Notice that $\lambda_{\min}(H_b H_b^\top) \neq 0$, as H_b has full row-rank, see Lemma 17.i). Consequently, for $t \in [t_0, t_1]$, the derivative of V satisfies

$$\frac{d}{dt}V(x) \leq -\left(\gamma \rho_{\mathbf{M}} - \overline{\xi}\|H_b\| - \frac{\sqrt{c}\|H_b\|\lambda_{\max}(R)\|C_2\|\kappa(H_b)}{2N\sqrt{\lambda_{\min}(P)}} \right) \|(\Theta_b^\top \otimes I_p) w\| \tag{27}$$

It follows from (24) that for $t \in [t_0, t_1]$, V is a non-increasing function and therefore $x(t_1) \in \operatorname{int} \Omega_c$. Following an induction argument, we conclude that for all $t \geq t_0$, $x(t) \in \Omega_c$, that is, Ω_c is a positively invariant set of the closed-loop (7)-(8). Finally, it follows from (27) that $(\Theta_b^\top \otimes I_p) w \to 0$ and the zero-state detectability assumption guarantees that $(\Theta_b^\top \otimes I_p) x \to 0$. That is, $\operatorname{dist}(x(t); \mathcal{S}) \to 0$ whenever $x(t) \in \mathcal{B}_{s(c)}(0) \subset \Omega_c$, where $s(c) = \frac{c}{N\lambda_{\min}(P)}$, and semi-global asymptotic synchronization follows.

Corollary 10 allows for designs when the subgraph $\mathcal{G}_a$ does not provide sufficient energy dissipation to achieve global synchronization. In such a case, the set-valued subnetwork induced by $\mathcal{G}_b$ is used to compensate the lack of dissipation by achieving a trade-off between the size of the region of attraction, estimated by Ω_c, and the size of the gain γ. Note that the bound on the gain γ in (24) depends on the number of agents N and the condition number of the matrix H_b. The latter can be interpreted as a measure of *how far* is $\mathcal{G}_b$ from the complete graph $\mathcal{K}_N$. Thus, smaller values of γ can be obtained by increasing either the number of vertices or the number of edges in $\mathcal{G}_b$.

It is also worth to remark that if $\lambda_{\max}(R) \leq 0$ in (23) then (25) together with the zero-state detectability assumption imply that the network (7) with coupling law (8) achieves global asymptotic synchronization.

5 Practical synchronization via regularization of ideal set-valued couplings

For achieving perfect regulation, as stated in Theorem 8 or Corollary 10, it is necessary to know the *exact* values (selection) of the control u in the set $\mathbf{M}(0)$ that will counteract the affection caused by the matched disturbances. Even though such scenario is unreal, the usefulness of Theorem 8 amounts to guide us in the design of regularized controllers achieving *approximate* selections. For differential inclusions with maximal monotone maps, there are two main approaches for regularization, that is, *a*) implicit discretization schemes and *b*) use of Lipschitz continuous approximate selections. Here we focus on the second approach.

Our choice over Lispchitz continuous approximate selections is motivated by the mechanisms envisaged for implementing the coupling signals. Namely, implicit discretization is commonly applied for a "chattering free" digital implementation of set-valued maximal monotone maps in regulatory control tasks, see *e.g.*, [21], [27], [40]. An alternative way to implement set-valued maps consists in using analog circuitry. For instance, let us consider the analog circuit in Figure 2 where each diode satisfies an ideal complementarity relation as,

$$0 \leq I_{D_k} \perp V^* - V_{D_k} \geq 0 \,, \tag{28}$$

where the notation $0 \leq a \perp b \geq 0$ stands for the following three conditions: i) $a \geq 0$, ii) $b \geq 0$ and iii) $ab = 0$, I_{D_k}, V_{D_k} denote the current through and the voltage across the k-th diode, respectively, and V^* denotes the activation voltage of the diode. In real-life circuits, each diode will have parasitic resistance effects even when in conduction mode.

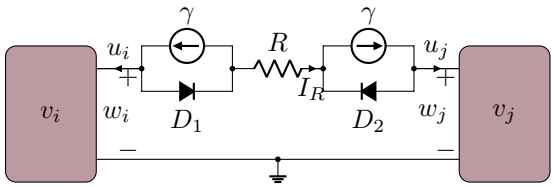

Fig. 2. Analog circuit implementation of an approximate selection to the set-valued coupling law $u_i = -u_j \in \gamma\mathbf{Sgn}(w_j - w_i)$.

Such resistances are considered as lumped in the resistor R. It follows from Kirchhoff's laws that the voltage-current relation of the coupling circuit satisfies,

$$-u_i = u_j = I_{D_1} - \gamma = \gamma - I_{D_2} \tag{29a}$$
$$w_i - w_j = \vartheta + RI_R \tag{29b}$$
$$\vartheta = V_{D_1} - V_{D_2} \tag{29c}$$
$$0 \leq I_{D_1} \perp V^* - V_{D_1} \geq 0 \tag{29d}$$
$$0 \leq I_{D_2} \perp V^* - V_{D_2} \geq 0 \tag{29e}$$

It follows from (29d)-(29e) and (29a) that, regardless of the value of V_a and V_b, $(u_i, u_j) \in [-\gamma, \gamma] \times [-\gamma, \gamma]$. Moreover, we have the following three cases,

i) $u_j = -\gamma$. It follows from (29a) that $I_{D_2} > 0$ and (29e) implies that $V^* - V_{D_2} = 0$. Hence, (29c) and (29d) imply that $\vartheta \in (-\infty, 0]$.
ii) $u_j = \gamma$. It follows from (29a) that $I_{D_1} > 0$ and (29d) implies that $V^* - V_{D_1} = 0$. Hence, (29c) and (29e) imply that $\vartheta \in [0, +\infty)$.
iii) $-\gamma < u_j < \gamma$. It follows from (29a) that $I_{D_1} > 0$ and $I_{D_2} > 0$. Hence the complementarity conditions (29d)-(29e) imply that $V^* - V_{D_1} = V^* - V_{D_2} = 0$ and it follows from (29c) that $\vartheta = 0$.

It is not difficult to see that the three cases above characterize the relation $\vartheta \in \mathbf{N}_{[-\gamma,\gamma]}(u_j)$. Equivalently, $u_j \in \gamma\mathbf{Sgn}(\vartheta)$. Hence, it follows from (29b), the fact that $I_R = u_j$, and (2) that

$$\vartheta = \mathcal{J}_{R\gamma\mathbf{Sgn}}\left(w_i - w_j\right) \tag{30}$$

Finally, the substitution of (30) back into (29b) leads us to,

$$\begin{aligned} -u_i = u_j &= \frac{1}{R}\left(w_i - w_j - \mathcal{J}_{R\gamma\mathbf{Sgn}}\left(w_i - w_j\right)\right) \\ &= \gamma \mathcal{Y}^{R\gamma}_{\mathbf{Sgn}}(w_i - w_j) \end{aligned}$$

where $\mathcal{Y}^{\varepsilon}_{\mathbf{M}}$ is the Yosida approximation of $\mathbf{M}$ of index $\varepsilon > 0$ given by (1). Therefore, the coupling circuit in Figure 2 implements a Lipschitz continuous approximate selection of the set-valued map **Sgn**. Note that in the limiting case where $R = 0$, the relations $\vartheta = w_i - w_j$ and $-u_i = u_j \in \gamma\mathbf{Sgn}(w_i - w_j)$ hold, leading to an ideal set-valued coupling.

In what follows we study how synchronization is affected by considering couplings given by Yosida approximations.

Corollary 11 *Let all the assumptions of Theorem 8 hold and consider the regularized coupling*

$$u = -(\Theta_a W \Theta_a^\top \otimes I_p)w - \gamma(\Theta_b \otimes I_p)\mathcal{Y}^{\varepsilon}_{\mathbf{M}}\left((\Theta_b^\top \otimes I_p)w\right) \ . \tag{31}$$

Then the asymptotic behavior of the network (7) *with coupling* (31) *is practically synchronized. Moreover, an estimation of the ultimate bound is given by the set*

$$\Omega_\varepsilon = \left\{ x \in \mathbb{R}^{Nn} | V(x) \leq \frac{\varepsilon\overline{\xi}\|H_b\|}{\mu} \right\} \ , \tag{32}$$

where μ, $\overline{\xi}$, and H_b are the same as in Theorem 8.

PROOF. Taking the Lyapunov function candidate (13), simple computations, similar to those made in the proof of Theorem 8, lead us to

$$\begin{aligned} \frac{d}{dt}V(x) \leq &-\frac{\mu}{2N}x^\top\left(\Theta_c\Theta_c^\top \otimes P\right)x - \gamma w^\top(\Theta_b \otimes I_p)\mathcal{Y}^{\varepsilon}_{\mathbf{M}}\left((\Theta_b^\top \otimes I_p)w\right) \\ &+ \overline{\xi}\|H_b\|\|(\Theta_b^\top \otimes I_p)w\| \end{aligned} \tag{33}$$

where μ and H_b are the same as in the proof of Theorem 8. Now, the substitution of (3) into (33) yields,

$$\begin{aligned} \frac{d}{dt}V(x) \leq -\mu V(x) + \overline{\xi}\|H_b\|\|(\Theta_b^\top \otimes I_p)w\| - \gamma\mathcal{J}_{\varepsilon\mathbf{M}}\left((\Theta_b^\top \otimes I_p)w\right)^\top \mathcal{Y}^{\varepsilon}_{\mathbf{M}}\left((\Theta_b^\top \otimes I_p)w\right) \\ - \varepsilon\gamma\|\mathcal{Y}^{\varepsilon}_{\mathbf{M}}\left((\Theta_b^\top \otimes I_p)w\right)\|^2 \end{aligned} \tag{34}$$

It follows from (4) and Lemma 18.i) that

$$\frac{d}{dt}V(x) \leq -\mu V(x) - \gamma\rho_{\mathbf{M}}\|\mathcal{J}_{\varepsilon\mathbf{M}}\left((\Theta_b^\top \otimes I_p)w\right)\| - \varepsilon\gamma\|\mathcal{Y}^{\varepsilon}_{\mathbf{M}}((\Theta_b^\top \otimes I_p)w)\|^2 + \overline{\xi}\|H_b\|\|(\Theta_b^\top \otimes I_p)w\| \tag{35}$$

Using, once again, (3) together with the triangle inequality in the second term of (35), leads us to

$$\frac{d}{dt}V(x) \leq -\mu V(x) - \left(\gamma\rho_{\mathbf{M}} - \overline{\xi}\|H_b\|\right)\|(\Theta_b^\top \otimes I_p)w\| - \varepsilon\gamma\left(\|\mathcal{Y}^{\varepsilon}_{\mathbf{M}}\left((\Theta_b^\top \otimes I_p)w\right)\| - \rho_{\mathbf{M}}\right)\|\mathcal{Y}^{\varepsilon}_{\mathbf{M}}((\Theta_b^\top \otimes I_p)w)\| \tag{36}$$

It follows from Lemma 18.ii) and (12) that the right-hand side of (36) is strictly negative whenever $\|(\Theta_b^\top \otimes I_p)w\| \notin \varepsilon\mathcal{B}_{\rho_{\mathbf{M}}}(0)$. Now assume that $(\Theta_b^\top \otimes I_p)w \in \varepsilon\mathcal{B}_{\rho_{\mathbf{M}}}(0)$ but $x \notin \Omega_\varepsilon$. In such case it follows again from Lemma 18.ii) that

$$\|\mathcal{Y}^{\varepsilon}_{\mathbf{M}}\left((\Theta_b^\top \otimes I_p)w\right)\| = \frac{\|(\Theta_b^\top \otimes I_p)w\|}{\varepsilon} \ .$$

and (36) becomes,

$$\frac{d}{dt}V(x) \leq -\mu V(x) - (\gamma\rho_{\mathbf{M}} - \overline{\xi}\|H_b\|)\|(\Theta_b^\top \otimes I_p)w\| - \varepsilon\gamma\left(\frac{\|(\Theta_b^\top \otimes I_p)w\|}{\varepsilon} - \rho_{\mathbf{M}}\right)\frac{\|(\Theta_b^\top \otimes I_p)w\|}{\varepsilon}$$
$$\leq -\mu\left(V(x) - \frac{\varepsilon\overline{\xi}\|H_b\|}{\mu}\right) - \frac{\gamma}{\varepsilon}\|(\Theta_b^\top \otimes I_p)w\|^2 \tag{37}$$

It follows from (36) and (37) that, whenever $x \notin \Omega_\varepsilon$, $V(x)$ is strictly decreasing. Therefore, $\text{dist}(x;\Omega_\varepsilon) \to 0$ as $t \to \infty$. Finally, noting that $\Omega_\varepsilon \subset \mathcal{N}_{r(\frac{1}{\varepsilon})}(\mathcal{S})$, where $\mathcal{N}_{r(\frac{1}{\varepsilon})}(\mathcal{S})$ is a neighborhood of the synchronization manifold $\mathcal{S}$, with $r(\frac{1}{\varepsilon}) = \sqrt{\frac{\varepsilon\overline{\xi}\|H_b\|}{\mu\lambda_{\min}(P)}}$ so that $r(\frac{1}{\varepsilon}) \to 0$ as $\frac{1}{\varepsilon} \to \infty$, then global practical synchronization follows.

From the proof of Corollary 11 it becomes clear that in order to have high precision in the presence of matched disturbances, it is better to look for a Yosida approximation with small index ε, (equivalently, a Yosida approximation with high incremental gain $1/\varepsilon$), rather than increasing the gain γ.

Example 12 *As an illustration, let us consider an heterogeneous group of $N = 32$ FitzHugh-Nagumo oscillators with agent dynamics* (5) *and parameters given by,*

$$A = \begin{bmatrix} 0 & -2 \\ \frac{1}{\delta} & \frac{0.1}{\delta} \end{bmatrix}, B_1 = B_2 = \begin{bmatrix} 1 \\ 0 \end{bmatrix}, C_1 = \begin{bmatrix} 1 & 0 \end{bmatrix}, \tag{38}$$

where $\delta = 0.05$, the matrix C_2 is defined below, and each agent v_k is closed with a distinct nonlinear feedback $\varphi_k : \mathbb{R} \to \mathbb{R}$, $\varphi_k(\eta) = \eta^3 - \alpha_k\eta$, where each constant α_k is selected in a random way from the interval $[2.5, 10]$. In addition, each agent is affected by external disturbances of the form $\xi_k = 2\cos(\beta_k t)\sin(x_{k,1}) + 2\sin(kx_{k,1})\cos(\sqrt{k}x_{k,2})$, where each constant β_k is selected randomly from the interval $[15, 20]$. Note that extra disturbances will appear due to the heterogeneity between agents. Indeed, it follows from simple computations that for any $\{i, j\} \in \mathcal{E}_c$

$$\varphi_i(y_i) - \varphi_j(y_j) = \frac{\varphi_i(y_i) - \varphi_i(y_j)}{2} + \frac{\varphi_j(y_i) - \varphi_j(y_j)}{2} + \frac{\varphi_i(y_i) - \varphi_j(y_i) + \varphi_i(y_j) - \varphi_j(y_j)}{2}$$
$$= \overline{\varphi}_{i,j}(y_i) - \overline{\varphi}_{i,j}(y_j) + \frac{(\alpha_j - \alpha_i)(y_i + y_j)}{2}, \tag{39}$$

where $\overline{\varphi}_{i,j} = \frac{\varphi_i + \varphi_j}{2}$. Moreover, for any $\{i, j\} \in \mathcal{E}_c$, the map $\overline{\varphi}_{i,j}$ satisfies (6) *on any compact set for appropriate values of K_1 and K_2. Namely, setting $\Delta\overline{\varphi}_{i,j} = \overline{\varphi}_{i,j}(y_i) - \overline{\varphi}_{i,j}(y_j)$ and $\Delta_{i,j}y = y_i - y_j$, then for any two $y_i, y_j \in \mathcal{B}_s(0)$, $s > 0$, direct calculations lead us to*

$$(\Delta\overline{\varphi}_{i,j} - K_1\Delta_{i,j}y)(\Delta\overline{\varphi}_{i,j} - K_2\Delta_{i,j}y) = \left(y_i^3 - y_j^3 - \left(\frac{\alpha_i + \alpha_j}{2} + K_1\right)\Delta_{i,j}y\right)\left(y_i^3 - y_j^3\left(\frac{\alpha_i + \alpha_j}{2} + K_2\right)\Delta_{i,j}y\right)$$
$$= \left(p(y_i, y_j) - \frac{\alpha_i + \alpha_j}{2} - K_1\right)\left(p(y_i, y_j) - \frac{\alpha_i + \alpha_j}{2} - K_2\right)(\Delta_{i,j}y)^2 \tag{40}$$

where $p(y_i, y_j) = y_i^2 + y_iy_j + y_j^2$. Since $0 \leq p(y_i, y_j) \leq 3s^2$ for all $y_i, y_j \in \mathcal{B}_s(0)$, it follows that $\overline{\varphi}_{i,j}$ satisfies (6) *in $\mathcal{B}_s(0)$ whenever,*

$$K_1 \leq \min_{\{i,j\}\in\mathcal{E}_c}\left\{-\frac{\alpha_i + \alpha_j}{2}\right\} \tag{41}$$

$$\max_{\{i,j\}\in\mathcal{E}_c}\left\{3s^2 - \frac{\alpha_i + \alpha_j}{2}\right\} \leq K_2\,. \tag{42}$$

Taking the same Lyapunov function candidate and following the same steps as in the proof of Theorem 8, mutatis

mutandis, *it follows that if* P *satisfies* (11) *we arrive at,*

$$\frac{d}{dt}V(x) \leq -\mu V(x) - \gamma w^\top(\Theta_b^\top \otimes I_p)\mathcal{Y}_{\mathbf{M}}^{\varepsilon}\left((\Theta_b^\top \otimes I_p)w\right) + \|H_b\|\left(\overline{\xi} + \frac{\tilde{\xi}(y)\sqrt{E_c}}{N}\right)\|(\Theta_b \otimes I_p)w\| \tag{43}$$

where $\tilde{\xi}(y) = \max_{\{i,j\}\in\mathcal{E}_c}|(\alpha_j - \alpha_i)(y_i + y_j)/2|$. *Therefore, if* γ *satisfies*

$$\gamma \geq \|H_b\|\left(\frac{\overline{\xi}}{\rho_{\mathbf{M}}} + \frac{\tilde{\xi}(y)\sqrt{E_c}}{N}\right), \tag{44}$$

then semi-global practical synchronization follows.

The same conclusion (with different ultimate bound and region of attraction) is obtained if we consider instead the assumptions of Corollary 10. In that case, γ *must satisfy,*

$$\gamma \geq \|H_b\|\left(\frac{\overline{\xi}}{\rho_{\mathbf{M}}} + \frac{\sqrt{c}\lambda_{\max}(R)\|C_2\|\kappa(H_b)}{2\rho_{\mathbf{M}}N\sqrt{\lambda_{\min}(P)}} + \frac{\tilde{\xi}(y)\sqrt{E_c}}{N}\right) \tag{45}$$

where $c > 0$ *is such that* (22) *holds.*

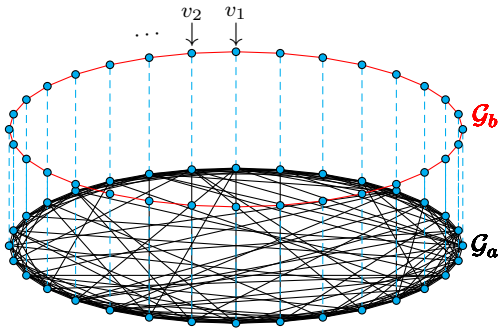

Fig. 3. Network structure induced by the coupling law (31). The black lines portray the network induced by Θ_a, where linear diffusion acts, whereas the red lines portray the network induced by Θ_b, where the nonlinear regularized coupling acts.

We now proceed to describe the structure of the network $\mathcal{G}(\mathcal{V},\mathcal{E})$ *together with the layers* $\mathcal{G}_a$ *and* $\mathcal{G}_b$ *of* (31). *The information available to each agent is described by a so-called small-world network of type Newman-Watts-Strogatz, where each vertex is connected to its* $k = 8$ *nearest neighboors and with probability of extra connections of* $p = 0.45$, *see [30] for details. The coupling configuration* (31) *is outlined in Figure 3, where* $\mathcal{G}_a$ *is the same as* $\mathcal{G}$ *and the subnetwork* $\mathcal{G}_b$ *constitutes the ring of vertices from agent* v_1 *up to agent* v_N. *Thus, the nonlinear coupling acts only on a subnetwork of* $\mathcal{G}$.

Concerning the other parameters of the coupling law (31), *we set* $W = I_{E_a}$ *the identity matrix, so that* $\beta = 1$, *and* $\mathbf{M} = \mathbf{Sgn} \times \cdots \times \mathbf{Sgn}$ *the componentwise signum set-valued map, so that* $\rho_{\mathbf{M}} < 1$. *An explicit expression for the Yosida approximation of* $\mathbf{M}$ *of index* ε *is*

$$\mathcal{Y}_{\mathbf{M}}^{\varepsilon}(\eta) = \mathrm{Proj}\left(\frac{\eta}{\varepsilon}; [-1,1]^{E_b}\right),$$

where $\mathrm{Proj}(\bullet; S) : \mathbb{R}^{E_b} \to S$, *denotes the classical projection map onto the closed, convex set* S. *Also, it follows from the network configuration that,* $\lambda_a = 4.36$, $\|H_b\| = 28.85$, *and* $\kappa(H_b) = 28.85$.

We now look for the output matrix C_2 *such that* (11) *holds. For the case* $C_2 = C_1$, *with the set of parameters indicated above, the LMI* (11) *is unfeasible, whereas the relaxed LMI* (23) *has a solution with a minimal value of* $R = 736.14$ *and* $\lambda_{\min}(P) = 0.1$, *leading to a large value of the gain* γ *according to* (45). *Thus, in order to reduce*

the aforementioned conservativeness, we consider C_2 in (11) *as another variable. After standard operations (a loop transformation changing the incremental sector of φ to the incremental sector $[0, K_2-K_1]$, together with a congruence transformation in* (11)*), we arrive at the following LMI*

$$\begin{bmatrix} Q_{1,1} & B_1 - P^{-1}C_1^\top \tilde{K}^\top \\ B_1^\top - \tilde{K}C_1P^{-1} & -2I_m \end{bmatrix} \preceq 0$$

where $Q_{1,1} = P^{-1}(A+B_1K_1C_1)^\top + (A+B_1K_1C_1)P^{-1} - \beta\lambda_a B_2B_2^\top + \mu P^{-1}$ and $\tilde{K} = K_2 - K_1$. By setting $C_2 = B_2^\top P$ we recover the output matrix. In this case, with the parameters aforementioned, we obtain that $C_2 = [8.53,\ -0.21]$ with $\mu = 0.1$. Therefore, setting $\gamma > 28.85(\overline{\xi} + 0.98\tilde{\xi}(y))$ guarantees the semiglobal practical synchronization of the perturbed network.

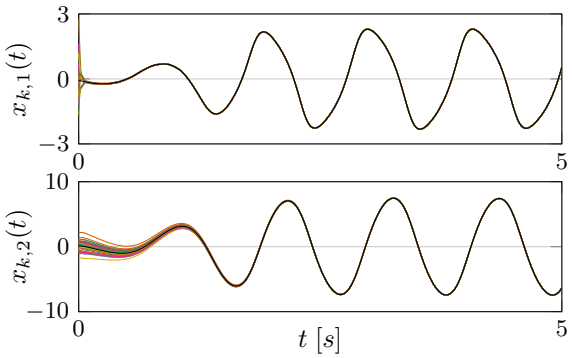

Fig. 4. Time evolution of states $x_{k,i}(t)$, $i \in \{1, 2\}$, of $N = 32$ distinct FitzHugh-Nagumo systems with monotone coupling (31) and $W = I_{E_a}$, $\gamma = 50$, $\mathbf{M} = \mathbf{Sgn}$ and $\varepsilon = 10^{-1}$. The black line represents the average behavior $\overline{x}(t)$.

Figure 4 shows the time trajectories of the state variables with the regularized controller (31) *with $\varepsilon = 10^{-1}$. The time evolution of the coupling signals is shown in the uppert part of Figure 5 for two different regularizations ($\varepsilon = 10^{-1}$ and $\varepsilon = 10^{-3}$). It is noteworthy that the regularized part of the coupling signals compensate for the disturbance term ξ as verifed in the lower part of Figure 5. Finally, the sum of squares error signal,*

$$e_{sos}(t) = \sum_{k=1}^{N} \|x_k(t) - \overline{x}(t)\|^2 , \tag{46}$$

where, $\overline{x}(t)$ denotes the averaged behavior, that is, $\overline{x}(t) = \frac{1}{N}\sum_{k=1}^{N} x_k(t)$, is displayed in Figure 6 for four different regularizations, verifying the claimed practical synchronization of the network.

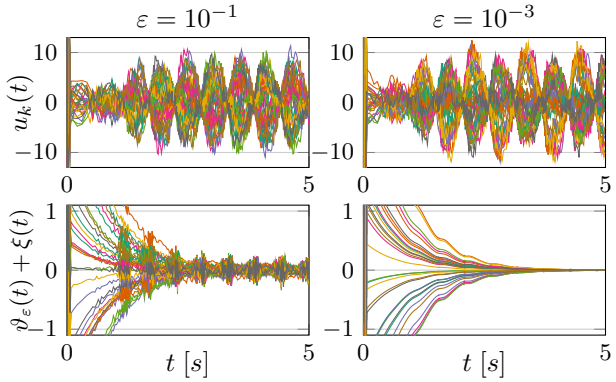

Fig. 5. Upper part: Time trajectories of coupling signals (31). Lower part: Time evolution of the difference $\vartheta_\varepsilon(t) + \xi(t)$, where $\vartheta_\varepsilon(t) = -(\Theta_b \otimes I_p)\mathcal{Y}^\varepsilon_{\mathbf{M}}\left((\Theta_b^\top \otimes I_p)w(t)\right)$, showing the compensation achieved by the regularized coupling acting on $\mathcal{G}_b$.

All simulations were performed with Python 3.0 using the Scipy function `solve_ivp` *with the solver* `BDF` *and* `rtol` $= 10^{-9}$. *The code is available via the link [26].*

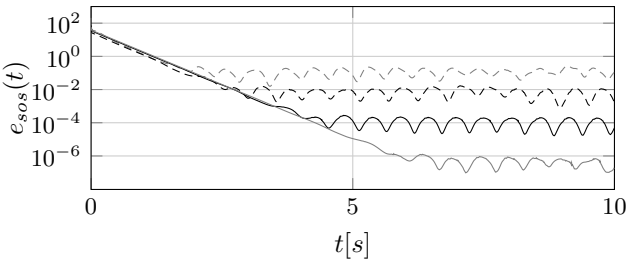

Fig. 6. Sum of squares error (46) of the network of $N = 32$ FitzHugh-Nagumo systems of Example 12 at four different regularizations: *a)* $\varepsilon = 10^0$ – dashed gray line; *b)* $\varepsilon = 10^{-1}$ – dashed black line; *c)* $\varepsilon = 10^{-2}$ – continuous black line; and *d)* $\varepsilon = 10^{-3}$ – continuous gray line. In all cases $W = I_{E_a}$ and $\gamma = 50$.

6 Synchronization under changes in network's topology

From the proof of Theorem 8 it is clear that the Lyapunov function $V(x) = x^\top(\Theta_c\Theta_c^\top \otimes P)x$ acts indeed as a Common Quadratic Lyapunov Function (CQLF), [25], for the family of networks with N vertices and connected graphs. Thereby, the previous developments easily extend to the case of networks in which the graph topology changes with time.

Let $G_N \subset \mathbb{N}$ be the set of indices enumerating all possible graphs with N vertices and let $\tilde{a} : \mathbb{R}_+ \to G_N$, $\tilde{b} : \mathbb{R}_+ \to G_N$, be right-continuous piecewise constant signals indexing the spanning subgraphs of $\mathcal{G}(\mathcal{V}, \mathcal{E})$ at time t. That is, there is a sequence $\{t_k^*\}_{k\in\mathbb{N}}$ such that for all $t \in [t_k^*, t_{k+1}^*)$, $\mathcal{G}_{\tilde{a}(t)}$ and $\mathcal{G}_{\tilde{b}(t)}$ are constant. Let us consider the matrix $\tilde{\Theta}_{\tilde{b}(t)} := [\Theta_{\tilde{b}(t)}, 0] \in \mathbb{R}^{N\times E_c}$, and consider the following coupling law

$$u(t) \in -(\Theta_{\tilde{a}(t)} W_{\tilde{a}(t)} \Theta_{\tilde{a}(t)}^\top \otimes I_p)w(t) - \gamma(\tilde{\Theta}_{\tilde{b}(t)} \otimes I_p)\mathbf{M}\left((\tilde{\Theta}_{\tilde{b}(t)}^\top \otimes I_p)w(t)\right) , \tag{47}$$

where $W_{\tilde{a}(t)} \in \mathbb{R}^{E_{\tilde{a}(t)}\times E_{\tilde{a}(t)}}$ is such that $\beta_{\min} := \min_{t,i}([W_{\tilde{a}(t)}]_{i,i}) > 0$ and $\mathbf{M} : \mathbb{R}^{E_c} \rightrightarrows \mathbb{R}^{E_c}$ is maximal monotone.

Corollary 13 *Let Assumptions 1-2 and 7 hold and let $\mathcal{G}_{\tilde{a}(t)}$ and $\mathcal{G}_{\tilde{b}(t)}$ be connected graphs for almost all times $t \geq t_0$. If,*

i) there exist $\mu > 0$ and a constant matrix $P = P^\top \succ 0$, satisfying the conditions of Corollary 6 uniformly in t, together with (11) with $\beta\lambda_a$ substituted by $\beta_{min}\tilde{\lambda}_a$, where $\tilde{\lambda}_a$ is the minimum connectivity of the finite family of all possible connected subgraphs $\{\mathcal{G}_{a_j}\}_{j\in G_N}$; and

ii) the gain $\gamma > 0$ is such that

$$\gamma > \frac{\overline{\xi}\tilde{H}}{\rho_{\mathbf{M}}} , \tag{48}$$

where $\tilde{H} = \max_t \|\tilde{H}_{\tilde{b}(t)}\|$ and $\tilde{H}_{\tilde{b}(t)}$ is such that $\Theta_c = \tilde{\Theta}_{\tilde{b}(t)}\tilde{H}_{\tilde{b}(t)}$ for almost all $t \geq t_0$.

Then the nonlinear network (7) with coupling (47) achieves global asymptotically synchronization.

PROOF. The proof is omitted since it is very similar to that of Theorem 8. Indeed, as the set G_N contains a finite number of elements and the subgraphs $\mathcal{G}_{\tilde{a}(t)}$ and $\mathcal{G}_{\tilde{b}(t)}$ are connected for almost all t, it follows that $\tilde{\lambda}_a > 0$ for almost all $t \geq t_0$. Now, using the CQLF candidate (13), together with Lemma 17, and following the same steps as in the proof of Theorem 8, we arrive at the analogue of (15), that is,

$$w^\top\left(\Theta_{\tilde{a}(t)} W_{\tilde{a}(t)} \Theta_{\tilde{a}(t)}^\top \otimes I_p\right) w \geq \frac{\beta_{\min}\tilde{\lambda}_a}{N} x^\top\left(\Theta_c\Theta_c^\top \otimes C_2^\top C_2\right) x . \tag{49}$$

Finally, mimicking the rest of the proof of Theorem 8 leads us to the claimed synchronization.

Similar results, dealing with *local* synchronization for the case of slowly varying connections, have been reported in [44] under the framework of the Master Stability Function (MSF), see *e.g.*, [33]. It is worth to remark that the

MSF formalism requires an explicit knowledge of the synchronized trajectory, which is inaccessible when considering unknown disturbances $\xi(t,x)$ as is the case treated in this work. By contrast, Corollary 13 provides a *global* approach for connected networks with time-varying coupling and extends the results presented in [6] to the case of heterogeneous networks with non-smooth coupling.

7 Beyond Filippov systems

In this section we consider set-valued maps not satisfying Assumption 7. For instance, let us consider the following modification of the coupling law (8),

$$u(t) \in -(\Theta_a W \Theta_a^\top \otimes I_p)w - (\Theta_b \otimes I_p)\mathbf{N}_{S(t)}((\Theta_b^\top \otimes I_p)w) \,, \tag{50}$$

where $\mathbf{N}_{S(t)}$ is the normal cone to the closed, convex, and time-dependent set $S(t) \subset \mathbb{R}^{E_b p}$. Hence, at each time t, $\mathbf{N}_{S(t)}$ is maximal monotone.

Assumption 14 *There exists an absolutely continuous function $\nu : [0,+\infty) \to \mathbb{R}$ such that for any $\eta \in \mathbb{R}^{Ep}$ and any $t_1, t_2 \in [0,+\infty)$*

$$|\mathrm{dist}(\eta, S(t_1)) - \mathrm{dist}(\eta, S(t_2))| \leq |\nu(t_1) - \nu(t_2)| \,, \tag{51}$$

Under Assumption 14 Theorem 5 can be modified to consider time-dependent maximal monotone operators, see [11, Theorem 23]. Thus, the existence and uniqueness of absolutely continuous solutions of the closed-loop (7), (50) is still guaranteed, whenever the initial condition satisfies $(\Theta_b^\top \otimes C_2)x(t_0) \in S(t_0)$. Such dynamical system is also known as a perturbed Moreau's sweeping process in the literature of contact dynamics [16], [37]. Our interest in Moreau's sweeping processes comes from the fact that well-posedness of the closed-loop, (7) with coupling (50), automatically implies that $(\Theta_b^\top \otimes I_p)w(t)$ belongs to the set $S(t)$ for almost all times $t > 0$. Thereby, *controlling* the time evolution of $S(t)$, leads to the control of the spatial mismatch $(\Theta_b^\top \otimes I_p)w(t)$. For instance, if $S(t) = [-s(t), s(t)]^{E_b p}$ is such that $0 < s(t) \to 0$ as $t \uparrow +\infty$ and $\mathcal{G}$ is connected, then $w(t) \to \mathrm{Null}(\Theta_b^\top \otimes I_p) = \mathrm{span}\{\mathbf{1}_N \otimes I_p\}$, and asymptotic synchronization follows by Assumption 3. It is worth to remark that, with the coupling law (50), the closed-loop system lies outside Filippov's framework, as $\mathbf{N}_{S(t)}$ is not a bounded set-valued map, (see Figure 1), a necessary condition for building Filippov's solutions, see *e.g.*, [17].

As in the case of the sign set-valued coupling, it is also possible to design electrical networks implementing a regularized version of the normal cone map in (50). Indeed, an analysis similar to the one done in Section 5, shows that the circuit on Figure 7 implements,

$$-u_i = u_j = \mathcal{Y}^{\varepsilon}_{\mathbf{M}_t^{-1}}(w_i - w_j) \,,$$

where $\mathbf{M}_t^{-1} = \mathbf{N}_{[-s(t),s(t)]}$, $s(t) = s^*(t) + V^*$, V^* is the activation voltage of the diodes, and $\varepsilon = R$.

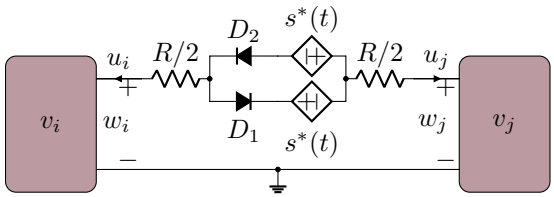

Fig. 7. Electrical network implementing a regularization of the set-valued map $-u_i = u_j \in \mathbf{N}_{[-s(t),s(t)]}(w_i - w_j)$, where $s(t) = s(t)^* + V^*$.

Corollary 15 *Let $S(t) = [-s(t), s(t)]^{E_b p}$ be the hypercube in $\mathbb{R}^{E_b p}$ with side length $2s(t)$ and centered at the origin, where $s : \mathbb{R}_+ \to \mathbb{R}_+$ is a strictly decreasing function such that $0 < s(t)$ for all $t \in [0,+\infty)$ and Assumption 14 holds. In addition let the initial condition $x(t_0) = x_0$ be such that $(\Theta^\top \otimes C_2)x_0 \in S(t_0)$. If condition i) of Corollary 10 holds, then the ensemble of systems (5) with regularized coupling law,*

$$u(t) = -(\Theta_a W \Theta_a^\top \otimes I_p)w - (\Theta_b \otimes I_m)\mathcal{Y}^{\varepsilon}_{\mathbf{M}_t^{-1}}\left((\Theta_b^\top \otimes I_p)w\right) \,, \tag{52}$$

where $\mathbf{M}_t^{-1} = \mathbf{N}_{S(t)}$*, achieves global practical synchronization whenever* $\varepsilon > 0$ *satisfies*

$$\frac{1}{\varepsilon} - \frac{\lambda_{\max}(R)\|H_b\|^2}{2N} - \frac{\overline{\xi}\|H_b\|}{\delta} > 0 \tag{53}$$

where the matrices R *and* H_b *are as specified in Corollary 10 and* $\delta > 0$ *is such that*

$$\|(\Theta_b \otimes I_p)w(t)\| > \delta \, .$$

PROOF. Consider once again the Lyapunov function (13). Simple computations leads us to the following inequality, *cf.* (25),

$$\begin{aligned}\frac{d}{dt}V(x) \leq \frac{\lambda_{\max}(R)\|H_b\|^2}{2N}\|(\Theta_b^\top \otimes I_p)w\|^2 - w^\top(\Theta_b \otimes I_p)\mathcal{Y}^{\varepsilon}_{\mathbf{M}_t}\left((\Theta_b^\top \otimes I_p)w\right) \\ + \overline{\xi}\|H_b\|\|(\Theta_b^\top \otimes I_p)w\| \, .\end{aligned} \tag{54}$$

The use of (3) and Lemma 19 in the Appendix leads us to

$$\begin{aligned}\frac{d}{dt}V(x) \leq -\left(\frac{1}{\varepsilon} - \frac{\lambda_{\max}(R)\|H_b\|^2}{2N}\right)\|(\Theta_b^\top \otimes I_p)w\|^2 + \frac{s(t)}{\varepsilon}w^\top(\Theta_b \otimes I_p)\mathcal{Y}^{\frac{s(t)}{\varepsilon}}_{\mathbf{M}}\left(\frac{(\Theta_b^\top \otimes I_p)w}{\varepsilon}\right) \\ + \overline{\xi}\|H_b\|\|(\Theta_b^\top \otimes I_p)w\| \, ,\end{aligned} \tag{55}$$

where $\mathbf{M} = \mathbf{Sgn} \times \cdots \times \mathbf{Sgn}$. It follows from (4) that $\|\mathcal{Y}^{\frac{s(t)}{\varepsilon}}_{\mathbf{M}}\left(\frac{(\Theta_b^\top \otimes I_p)w}{\varepsilon}\right)\| \leq \sqrt{E_b p}$. Hence, for any $\delta > 0$ such that $\|(\Theta_b^\top \otimes I_p)w\| \geq \delta$, it follows from (55) that

$$\frac{d}{dt}V(x) \leq -\left(\frac{1}{\varepsilon} - \frac{\lambda_{\max}(R)\|H_b\|^2}{2N} - \frac{s(t)\sqrt{E_b p}}{\delta\varepsilon} - \frac{\overline{\xi}\|H_b\|}{\delta}\right)\|(\Theta_b^\top \otimes I_p)w\|^2 \, . \tag{56}$$

Since $s(t) \downarrow 0$ as $t \uparrow \infty$, it follows from (53) that there exists a finite time $\tau^* > 0$ from which the right-hand side of (56) becomes negative thereafter. Finally, the conclusion follows from Assumption 3 on the incremental asymptotic zero-state detectability of the network. This concludes the proof.

Generalized Moreau's sweeping processes have a non-empty intersection with the so-called funnel control studied in [7], [22], [24]. In that context, the set $S(t)$ specifies the funnel where the error $(\Theta_b^\top \otimes C_2)x(t)$ will lie. Such control method is also related to the dead-zone control studied in [12]. Indeed funnel control can be interpreted as a version of the control proposed in [12] with open-loop adaptation.

Example 16 *Consider an ensemble of* $N = 16$ *Chua's circuits, where the* k*-th agent has parameters*

$$A = \begin{bmatrix} -\alpha_k & \alpha_k & 0 \\ 1 & -1 & 1 \\ 0 & -\beta & 0 \end{bmatrix}, B_1 = B_2 \begin{bmatrix} 1 \\ 0 \\ 0 \end{bmatrix}, C_1 = C_2 \begin{bmatrix} 1 & 0 & 0 \end{bmatrix}$$

where $k \in \{1, \ldots, N\}$*,* $\alpha_k \in [8.0, 9.5]$*,* $\beta = 15.0$*, and* $\varphi_k : \mathbb{R} \to \mathbb{R}$ *is such that* $\eta \mapsto \alpha_k(c_k\eta + \tanh(d_k\eta))$*, where* $c_k \in [1.5, 2.5]$*,* $d_k \in [0.5, 0.9]$*. All parameters are assumed constant, but* α_k*,* c_k *and* d_k *are selected in a random fashion within the indicated intervals. In addition, there is an external disturbance,* ξ_k*, affecting each agent via* $\xi_k = \sin(\delta_{k,1}\pi t)\sin(\delta_{k,2}t)\cos(\delta_{k,3}t) + \cos(\delta_{k,4}t)\sin(\delta_{k,5}\pi t)$*, where* $\delta_{k,i} \in [1, 20]$*,* $i \in \{1, \ldots, 5\}$*,* $k \in \{1, \ldots, N\}$*. As before, each* $\delta_{k,i}$ *is fixed and selected randomly.*

As in Example 12, the differences between agents will produce extra disturbances to be considered. Indeed, one has that

$$\varphi_i(y_i) - \varphi_j(y_j) = \overline{\varphi}_{i,j}(y_i) - \overline{\varphi}_{i,j}(y_j) + \tilde{\xi}_{i,j} \tag{57}$$

where $\overline{\varphi}_{i,j} = \frac{\varphi_i+\varphi_j}{2}$ *satisfies* (6) *for all* $i,j \in \{1,\dots,N\}$, *with* $K_1 = \min_{i,j}\{\frac{\tilde{\alpha}_{i,j}}{2}\}$, $K_2 = \max_{i,j}\{\frac{\tilde{d}_{i,j}+\tilde{\alpha}_{i,j}}{2}\}$, $\tilde{\alpha}_{i,j} = \alpha_i c_i + \alpha_j c_j$, $\tilde{d}_{i,j} = \alpha_i d_i + \alpha_j d_j$ *and*

$$\tilde{\xi}_{i,j} = \frac{(\alpha_i c_i - \alpha_j c_j)(y_i + y_j) + \phi_{i,j}(y_i) - \phi_{i,j}(y_j)}{2} ,$$

where $\phi_{i,j}(\eta) = \alpha_i \tanh(d_i\eta) - \alpha_j \tanh(d_j\eta)$. *Regarding the network structure, this time we set* $\Theta_a = 0$ *and* $\Theta_b = \Theta_{\tilde{b}(t)}$, *that is the network contains only one layer and it changes as time progress. At time* $t = 0$, *we start with an initial small-world graph configuration of the same type as before with connectivity of* 4 *neighbors and probability of extra connections equal* 0.25, *see,* e.g., *[30]. After every two seconds, the graph topology changes as follows,* $p_{\tilde{b}(t)} \in [0, 8]$ *edges are removed in a random way, and* $q_{\tilde{b}(t)} \in [0, 8]$ *edges are added also in a random manner such that the resulting graphs are always connected.*

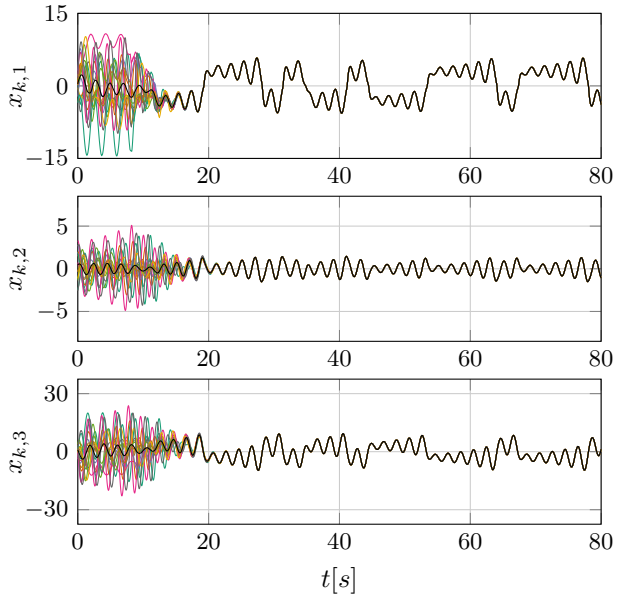

Fig. 8. Time trajectories of $N = 16$ heterogeneous Chua's circuits with coupling law (52) with $\mathbf{M}_t^{-1} = \mathbf{N}_{S(t)}$, $S(t) = [-50e^{-\frac{t^2}{50}}, 50e^{-\frac{t^2}{50}}]^{E_{\tilde{b}(t)}}$, and $\varepsilon = 0.01$. The black line represents the average behavior $\overline{x}(t)$ to which all trajectories converge.

Thereby, following similar steps to those shown in Example 12 we can conclude on the semi-global practical synchronization of the network. Indeed, with the above data each agent satisfies the LMI (23) *(uniformly in* α_k*), with* $\lambda_a = 0$, $P = Diag[1.0, 8.75, 0.58]$ *and* $R = 91.89$.

We use the coupling law (52) *with the set* $S(t) = [-50e^{\frac{-t^2}{50}}, 50e^{\frac{-t^2}{50}}]^{E_{\tilde{b}(t)}}$, *where* $E_{\tilde{b}(t)}$ *is the number of edges in* $\mathcal{G}_{\tilde{b}(t)}$. *An explicit formula for the regularized controller is*

$$\mathcal{Y}^{\varepsilon}_{\mathbf{M}_t^{-1}}(\vartheta) = \frac{\vartheta - \mathrm{Proj}(\vartheta; S(t))}{\varepsilon} , \tag{58}$$

Thus, as time increases, the set $S(t)$ *shrinks towards the origin and* $(\Theta_b^\top \otimes I_p)w(t)$ *approaches a neighborhood of the origin. It is also clear from* (58) *that the coupling action is zero whenever* $(\Theta_b^\top \otimes I_p)w(t) \in \mathrm{int}\, S(t)$. *This behavior is verified in Figures 16-16. Note that the control action remains bounded during the whole time of execution. As before, all simulations were performed with Python 3.0 using the Scipy function* `solve_ivp` *with the solver* `BDF` *and* `rtol` $= 10^{-9}$. *The code is available via the link [26].*

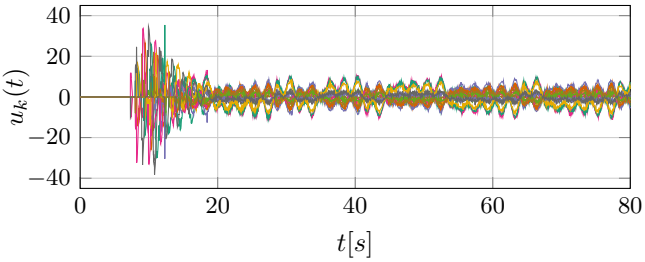

Fig. 9. Time evolution of the coupling law (52) with $\mathbf{M}_t^{-1} = \mathbf{N}_{S(t)}$, $S(t) = [-50e^{\frac{-t^2}{50}}, 50e^{\frac{-t^2}{50}}]^{E_{\tilde{b}(t)}}$, and $\varepsilon = 0.01$. From $t = 0$ up to $t \approx 8$ s, the coupling action is identically zero, indicating that $(\Theta_{\tilde{b}(t)} \otimes I_p)w \in \operatorname{int} S(t)$ during such time interval. Also note that all coupling signals remain bounded.

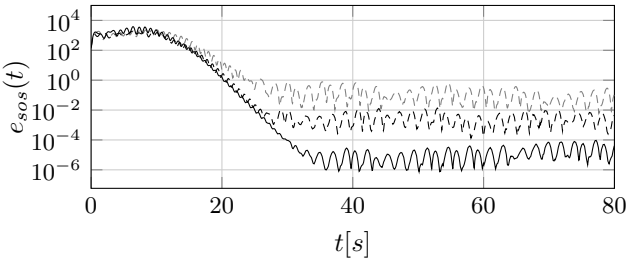

Fig. 10. Time trajectories for the sum of squares error signal $e_{sos}(t) = \sum_{k=1}^{N} \|x_k(t) - \overline{x}(t)\|^2$ for the family of $N = 16$ Chua's circuits with time-varying network connections and coupling law (52) with $\mathbf{M}_t^{-1} = \mathbf{N}_{[-s(t),s(t)]}$. The plot shows three different regularizations, *a*) $\varepsilon = 10^{-1}$ – dashed gray line; *b*) $\varepsilon = 10^{-2}$ – dashed black line; and *c*) $\varepsilon = 10^{-3}$ – continuous black line.

It is noteworthy that, due to the variability in the parameters, each perturbed agent in Example 16 has a different behavior. Indeed, most agents are not even in a chaotic regime due to the effects of each ξ_k. Thus, the average $\overline{x}(t) = \sum_{k=1}^{N} x_k(t)$ is not an individual solution for each agent. Nonetheless, the coupled system reaches practical synchronization towards a chaotic regime.

8 Conclusions and further research

The problem of robust synchronization against matched perturbations in the agents and uncertainty in network connections was dealt in this paper. It is shown that set-valued maximal monotone maps achieve perfect regulation in the presence of the aforementioned disturbances, but the *selection* of the coupling strategy depends on the disturbance itself and therefore perfect regulation is impossible to achieve in practice. Based on such knowledge, the regularization of the coupling law is explored via Yosida approximations. It is shown that practical synchronization is attained and precision improves as the index of the Yosida approximant approaches zero. Further research considers the digital implementation of the set-valued coupling via the time-discretization of the closed-loop system. In such regard, implicit discretization schemes have proved a superior performance and show a considerable reduction of the chattering effect, even when tested in physical systems, see *e.g.*, [21], [40].

References

[1] M. Arcak. Certifying spatially uniform behavior in reaction-diffusion PDE and compartmental ODE systems. *Automatica*, 47:1219–1229, 2011.

[2] H. Attouch and A. Damlamian. On multivalued evolution equations in Hilbert spaces. *Israel Journal of Mathematics*, 12:373–390, 1972.

[3] V. Barbu. *Nonlinear differential equations of monotone types in Banach spaces*. Springer, New York, USA, 2010.

[4] J. Bastien and M. Schatzman. Numerical precision for differential inclusions with uniqueness. *ESAIM: Mathematical Modelling and Numerical Analysis*, 36(3):427–460, 2002.

[5] H. H. Bauschke and P. L. Combettes. *Convex Analysis and Monotone Operator Theory in Hilbert Spaces*. CMS Books in Mathematics. Springer New York, 2011.

[6] I. V. Belykh, V. N. Belykh, and M. Hasler. Blinking model and synchronization in small-world networks with a time-varying coupling. *Physica D*, 195:188–206, 2004.

[7] T. Berger, A. Ilchmann, and E. P. Ryan. Funnel control of nonlinear systems. *Mathematics of Control, Signals, and Systems*, 33:151–194, 2021.

[8] S. Boccaletti, G. Bianconi, R Criado, C. I. del Genio, J. Gómez-Gardeñez, M. Romance, I. Sendiña Nadal, Z. Wang, and M. Zanin. The structure and dynamics of multilayer networks. *Physics Reports*, 544:1–122, 2014.

[9] H. Brézis. *Opérateurs Maximaux Monotones et Semi-groupes de Contractions dans les Espaces de Hilbert*. North-Holland Publishing Company, 1973.

[10] B. Brogliato and D. Goeleven. Well-posedness, stability and invariance results for a class of multivalued Lur'e dynamical systems. *Nonlinear Analysis: Theory, Methods and Applications*, 74(1):195–212, 2011.

[11] K. Camlibel, L. Iannelli, and A. Tanwani. Convergence of proximal solutions for evolution inclusions with time-dependent maximal monotone operators. *Mathematical programming*, 2021.

[12] G. Casadei, D. Astolfi, A. Alessandri, and L. Zaccarian. Synchronization in networks of identical nonlinear systems via dynamic dead zones. *IEEE Control Systems Letters*, 3(3):667–672, 2019.

[13] M. Coraggio, P. DeLellis, and M. di Bernardo. Convergence and synchronization in networks of piecewise-smooth systems via distributed discontinuous coupling. *Automatica*, 129:1–9, 2021.

[14] P. DeLellis, M. di Bernardo, T. E. Gorochowski, and G. Russo. Synchronization and control of complex networks via contraction, adaptation and evolution. *IEEE Circuits and Systems Magazine*, pages 64–82, 2010.

[15] P. DeLellis, M. di Bernardo, and D. Liuzza. Convergence and synchronization in heterogeneous networks of smooth and piecewise smooth systems. *Automatica*, 56:1–11, 2015.

[16] J. F. Edmond and L. Thibault. Relaxation of an optimal control problem involving a perturbed sweeping process. *Mathematical programming*, 104:347–373, 2005.

[17] A. F. Filippov and F. M. Arscott. *Differential Equations with Discontinuous Righthand Sides: Control Systems*. Mathematics and its Applications. Springer, 1988.

[18] C. Godsil and G. Royle. *Algebraic Graph Theory*. Springer, New York, USA, 2001.

[19] S. Gómez, A. Díaz-Guilera, J. Gómez-Gardeñez, C. J. Pérez-Vicente, Y. Moreno, and A. Arenas. Diffusion dynamics on multiplex networks. *Physical Review Letters*, 110:028701–1 – 028701–5, 2013.

[20] R. A. Horn and C. R. Johnson. *Matrix Analysis*. Cambridge University Press, New York, USA, second edition, 2013.

[21] O. Huber, V. Acary, and B. Brogliato. Lyapunov stability and performance analysis of the implicit discrete sliding mode control. *Automatic Control, IEEE Transactions on*, 2016.

[22] A. Ilchmann and E. P. Ryan. High-gain control without identification: a survey. *GAMM-Mitteilungen*, 31(1):115–125, 2008.

[23] J. G. Lee and R. Sepulchre. Rapid synchronization under weak synaptic coupling. In *59th IEEE Conference on Decision and Control (CDC)*, pages 6168–6173, Jeju Island, Republic of Korea, Dec. 2020.

[24] J. G. Lee, S. Trenn, and H. Shim. Synchronization with prescribed transient behavior: heterogeneous multi-agent systems under funnel coupling. *Automatica*, 141:110276, 2022.

[25] D. Liberzon. *Switching in Systems and Control*. Birkhäuser, New York, USA, 2003.

[26] F. A. Miranda-Villatoro. Python code for simulations. `https://gitlab.inria.fr/fmiranda/networksimulationsMaxMonotone`, 2022.

[27] F. A. Miranda-Villatoro, B. Brogliato, and F. Castaños. Multivalued robust tracking control of fully actuated Lagrange systems: Continuous and discrete-time algorithms. 2017.

[28] N. Monshizadeh, H. L. Trentelman, and M. K. Camlibel. Uniform synchronization in multi-agent systems with switching topologies. *International Journal of Robust and Nonlinear Control*, 26:1888–1901, 2015.

[29] J. M. Montenbruck, M. Bürger, and F. Allgöwer. Practical synchronization with diffusive couplings. *Automatica*, 53:235–243, 2015.

[30] M. E. J. Newman and D. J. Watts. Renormalization group analysis of the small-world network model. *Physics Letters A*, 263:341–346, 1999.

[31] R. Olfati-Saber, J. A. Fax, and R. M. Murray. Consensus and cooperation in networked multi-agent systems. *Proceeding of the IEEE*, 95(1):215–233, 2007.

[32] E. Panteley and A. Loría. Synchronization and dynamic consensus of heterogeneous networked systems. *IEEE Transactions on Automatic Control*, 62(8):3758–3773, 2017.

[33] L. M. Pecora and T. L. Carroll. Master stability functions for synchronized coupled systems. *Physical Review Letters*, 8(10):2019–2112, 1998.

[34] A. V. Proskurnikov, F. Zhang, M. Cao, and J. M. A. Scherpen. A general criterion for synchronization of incrementally dissipative nonlinear coupling agents. In *European Control Conference (ECC)*, pages 581–586, Linz, Austria, 2015.

[35] R. T. Rockafellar and R. J.-B. Wets. *Variational Analysis*. Springer-Verlag, 2009.

[36] L. Scardovi and R. Sepulchre. Synchronization in networks of identical linear systems. *Automatica*, 45:2557–2562, 2009.

[37] L. Thibault. Sweeping process with regular and nonregular sets. *Journal of Differential Equations*, 193:1–26, 2003.

[38] H. L. Trentelman, K. Takaba, and N. Monshizadeh. Robust synchronization of uncertain linear muti-agent systems. *International Journal of Robust and Nonlinear Control*, 58(6):1511–1523, 2013.

[39] V. Utkin, J. Guldner, and J. Shi. *Sliding Mode Control in Electro-Mechanical Systems*, volume 34. CRC press, 2009.

[40] B. Wang, B. Brogliato, V. Acary, A. Boubakir, and F. Plestan. Experimental comparisons between implicit and explicit implementations of discrete-time sliding mode controllers: Toward input and output chattering suppression. *IEEE Transactions on Control Systems Technology*, 23(5):2071–2075, 2015.

[41] W. Wang and J.-J. E. Slotine. On partial contraction analysis for coupled nonlinear oscillators. *Biological Cybernetics*, 92:2004, 2004.

[42] J. Zhao, D. J. Hill, and T. Liu. Synchronization of complex dynamical networks with switching topology: A switched system point of view. *Automatica*, 45:2502–2511, 2009.

[43] J. Zhao, D. J. Hill, and T. Liu. Global bounded synchronization of general dynamical networks with nonidentical nodes. *IEEE Transactions on Automatic Control*, 57(10):2656–2662, 2012.

[44] J. Zhou, Y. Zou, S. Guan, Z. Liu, and S. Boccaletti. Synchronization in slowly switching networks of coupled oscillators. *Nature Scientific Reports*, 6(35979), 2016.

A Appendix

Lemma 17 *Let $\Theta \in \mathbb{R}^{N\times E}$ be an oriented incidence matrix associated to a graph $\mathcal{G}(\mathcal{V},\mathcal{E})$ and let $\Theta_c \in \mathbb{R}^{N\times E_c}$, where $E_c = \frac{N(N-1)}{2}$, be an incidence matrix associated to the complete graph $\mathcal{K}_N$.*

i) If Θ has rank $N-1$, then there exists a full row-rank matrix $H \in \mathbb{R}^{E\times E_c}$ such that $\Theta_c = \Theta H$.
ii) $\Theta_c\Theta_c^\top\Theta = N\Theta$.

PROOF. i) Without loss of generality consider the case where the first E columns of Θ_c coincide with those of Θ. Since Θ has rank $N-1$, then for any edge $\{v_i, v_j\} \in \mathcal{E}_c$ there is a path in $\mathcal{G}$ joining v_i and v_j. Therefore, the remaining columns of Θ_c are a linear combination of columns of Θ. That is $\Theta_c = \Theta[I_E, T]$ for some $T \in \mathbb{R}^{E\times(E_c-E)}$. Setting $H = [I_E, T]$, clearly H has full row-rank and the claim follows.

ii) Let L_c be the Laplacian matrix of the complete graph $\mathcal{K}_N$, i.e., $L_c = \Theta_c\Theta_c^\top$ and let $r_j, s_j \in \{1,\dots,N\}$ be such that $[\Theta]_{r_j,j} = 1$ and $[\Theta]_{s_j,j} = -1$. Then, the j-th column of $L_c\Theta$ satisfies

$$[L_c\Theta]_{\bullet,j} = [L_c]_{\bullet,r_j} - [L_c]_{\bullet,s_j} = N[\Theta]_{\bullet,j}\ ,$$

and the conclusion follows.

Lemma 18 *Let $\mathbf{M}$ be a maximal monotone map satisfying Assumption 7. Then,*

i) For any $(\eta,\vartheta) \in \mathrm{gph}(\mathbf{M})$, $\eta^\top\vartheta \geq \rho_{\mathbf{M}}\|\eta\|$.
ii) For any $\varepsilon > 0$, $\|\mathcal{Y}^\varepsilon_{\mathbf{M}}(\vartheta)\| < \rho_{\mathbf{M}}$, if and only if, $\vartheta \in \mathrm{int}\,(\varepsilon\mathcal{B}_{\rho_{\mathbf{M}}}(0))$.

PROOF. i) Let $(\eta,\vartheta) \in \mathrm{gph}(\mathbf{M})$. It follows from the assumption on $\mathbf{M}(0)$ that $(0,\hat\vartheta) \in \mathrm{gph}(\mathbf{M})$, for all $\hat\vartheta \in \mathcal{B}_{\rho_{\mathbf{M}}}(0)$. Hence, monotonicity of $\mathbf{M}$ implies that,

$$\langle \eta, \vartheta - \hat\vartheta\rangle \geq 0 \text{ for all } \hat\vartheta \in \mathcal{B}_{\rho_{\mathbf{M}}}(0).$$

Therefore, $\langle\eta,\vartheta\rangle \geq \sup_{\hat\vartheta\in\mathcal{B}_{\rho_{\mathbf{M}}}(0)}\langle\eta,\hat\vartheta\rangle = \rho_{\mathbf{M}}\|\eta\|$, and the implication follows.

ii) Let $\vartheta \in \mathrm{int}\,(\varepsilon\mathcal{B}_{\rho_{\mathbf{M}}}(0))$. It follows from (2) that $\mathcal{J}_{\varepsilon\mathbf{M}}(\vartheta) = 0$. Hence, (3) implies that

$$\|\mathcal{Y}^\varepsilon_{\mathbf{M}}(\vartheta)\| = \frac{\|\vartheta - \mathcal{J}_{\varepsilon\mathbf{M}}(\vartheta)\|}{\varepsilon} = \frac{\|\vartheta\|}{\varepsilon} < \rho_{\mathbf{M}}\ .$$

For the converse, let $\vartheta \notin \mathrm{int}\,(\varepsilon\mathcal{B}_{\rho_{\mathbf{M}}}(0))$. In particular, $\vartheta \neq 0$, $\varepsilon\rho_{\mathbf{M}}\frac{\vartheta}{\|\vartheta\|} \in \varepsilon\mathcal{B}_{\rho_{\mathbf{M}}}(0) \subset \varepsilon\mathbf{M}(0)$, and $\mathcal{J}_{\varepsilon\mathbf{M}}\left(\varepsilon\rho_{\mathbf{M}}\frac{\vartheta}{\|\vartheta\|}\right) = 0$.

Thus, the nonexpansiveness property of the resolvant implies that

$$\begin{aligned}\|\mathcal{J}_{\varepsilon\mathbf{M}}(\vartheta)\| &= \left\|\mathcal{J}_{\varepsilon\mathbf{M}}(\vartheta) - \mathcal{J}_{\varepsilon\mathbf{M}}\left(\varepsilon\rho_{\mathbf{M}}\frac{\vartheta}{\|\vartheta\|}\right)\right\| \\ &\leq \left\|\vartheta - \varepsilon\rho_{\mathbf{M}}\frac{\vartheta}{\|\vartheta\|}\right\| = \|\vartheta\| - \varepsilon\rho_{\mathbf{M}}\,. \end{aligned} \tag{A.1}$$

Therefore,

$$\begin{aligned}\|\mathcal{Y}^{\varepsilon}_{\mathbf{M}}(\vartheta)\| &= \frac{1}{\varepsilon}\|\vartheta - \mathcal{J}_{\varepsilon\mathbf{M}}(\vartheta)\| \geq \frac{1}{\varepsilon}\left(\|\vartheta\| - \|\mathcal{J}_{\varepsilon\mathbf{M}}(\vartheta)\|\right) \\ &\geq \frac{1}{\varepsilon}\left(\|\vartheta\| - \|\vartheta\| + \varepsilon\rho_{\mathbf{M}}\right) = \rho_{\mathbf{M}}\end{aligned}$$

where we have made use of (A.1) in the last inequality, and the conclusion follows.

Lemma 19 *Let $S(t) = [-s(t), s(t)]^l \subset \mathbb{R}^l$ be such that $s(t) > 0$ for all $t \geq t_0$. That is, $S(t)$ is the hypercube in $\mathbb{R}^l$, with side length $2s(t)$ and centered at the origin. Let $\mathbf{M}_t^{-1} := \mathbf{N}_{S(t)}$. Then for any $\vartheta \in \mathbb{R}^l$, $\varepsilon > 0$ and $t \geq t_0$,*

$$\mathcal{Y}^{\varepsilon}_{\mathbf{M}_t^{-1}}(\vartheta) = \mathcal{J}_{\frac{s(t)}{\varepsilon}\mathbf{M}}\left(\frac{\vartheta}{\varepsilon}\right)\,, \tag{A.2}$$

$$\mathcal{J}_{\varepsilon\mathbf{M}_t^{-1}}(\vartheta) = s(t)\mathcal{Y}^{\frac{s(t)}{\varepsilon}}_{\mathbf{M}}\left(\frac{\vartheta}{\varepsilon}\right)\,, \tag{A.3}$$

where $\mathbf{M} : \mathbb{R}^l \rightrightarrows \mathbb{R}^l$ is the componentwise signum set-valued map, that is $\mathbf{M}(\eta) = \mathbf{Sgn}(\eta_1) \times \cdots \times \mathbf{Sgn}(\eta_l)$.

PROOF. The proof follows as a consequence of [35, Lemma 12.14]. Indeed, noting that $\mathbf{M}_t = s(t)\mathbf{M}$, it follows from (1) that

$$\begin{aligned}\eta = \mathcal{Y}^{\varepsilon}_{\mathbf{M}_t^{-1}}(\vartheta) &\Leftrightarrow \vartheta - \varepsilon\eta = \mathcal{J}_{\varepsilon\mathbf{M}_t^{-1}}(\vartheta) \\ &\Leftrightarrow \eta \in \mathbf{M}_t^{-1}(\vartheta - \varepsilon\eta) \\ &\Leftrightarrow \vartheta - \varepsilon\eta \in s(t)\mathbf{M}(\eta) \\ &\Leftrightarrow \frac{\vartheta}{\varepsilon} \in \eta + \frac{s(t)}{\varepsilon}\mathbf{M}(\eta) \\ &\Leftrightarrow \eta = \mathcal{J}_{\frac{s(t)}{\varepsilon}\mathbf{M}}\left(\frac{\vartheta}{\varepsilon}\right)\end{aligned} \tag{A.4}$$

and the identity (A.2) follows. Finally, the identity (A.3) follows as a consequence of (A.2) and (3).